Australian Government
Department of Defence
Defence Science and
Technology Organisation

Structural Risk Assessment of RAAF B707 Lower Wing Stringers

B. Dixon

Air Vehicles Division
DSTO Defence Science and Technology Organisation

DSTO-TR-1741

ABSTRACT

This report details a structural risk assesment of the critical lower wing stringers in RAAF B707 aircraft. The analysis uses condition data from sampling inspections of RAAF aircraft to describe possible cracking of these stringers in the fleet. It then uses crack growth and load exceedance data that has been adapted from a USAF risk assessment of the B707 to predict the future probability of failure of the B707 lower wing.

Published by

Air Vehicles Division
DSTO Defence Science and Technology Organisation
506 Lorimer St
Fishermans Bend, Victoria 3207 Australia

Telephone: (03) 9626 7000
Fax: (03) 9626 7999

AR-013-448
July 2005

APPROVED FOR PUBLIC RELEASE

Structural Risk Assessment of RAAF B707 Lower Wing Stringers

Executive Summary

The Royal Australian Air Force (RAAF) currently has a fleet of four active Boeing 707 (B707) aircraft. In the mid-1990s a United States Air Force (USAF) risk analysis identified four of the B707's lower wing stringers as high risk structural members. In response to the USAF analysis, DSTO performed its own assessment of the risk to RAAF aircraft. This analysis recommended the use of high frequency eddy current (HFEC) inspection around each fastener hole of the four stringers. Recently however, the RAAF has advised DSTO that inspection using HFEC on two of the critical stringers is a non preferred option. It has also advised that full coverage of the stringers during inspections is not possible.

As a result of this advice the structural risk assessment in this report was performed. The aim of the analysis was to show that the safety of the RAAF B707 could be maintained with current Boeing inspections. The analysis is a standard risk assessment using Monte Carlo simulations of the growth of cracks in the critical stringers. The initial condition of the stringers was estimated from the results of sampling inspections that were performed in 1999/2000. The growth of cracks in the stringers was estimated from the crack growth function used to grow cracks in the USAF B707 J-STARS risk analysis. The data in this risk analysis was also used as the basis of functions that were used to describe residual strength and the largest loads experienced in a flight. Where it was possible, the USAF data was adapted for RAAF usage.

The results of this report estimate the probability that the B707's lower wing will fail in a single flight. These estimates are made for future times and compared with standards of acceptable probability of failure to allow the RAAF take remedial actions before the risk level when flying their B707 aircraft becomes unacceptable.

Authors

B. Dixon
Air Vehicles Division

Mr Dixon graduated from the Royal Melbourne Institute of Technology with a Bachelor of Aerospace Engineering with Honours in 1998. He worked for Aerostructures Technologies on the F/A-18 IFOSTP fatigue test in 1998 and 1999. Since joining DSTO in 2002, he has worked in the risk and reliability field, primarily on the B707 and F/A-18 tasks. He is presently the test engineer for a program that involves the teardown and testing of ex-service F/A-18 centre barrels.

Contents

List of Tables

List of Figures

1. Introduction

The Royal Australian Air Force (RAAF) currently has a fleet of five Boeing 707 (B707) aircraft performing transport, training and air-to-air refuelling missions. The status of the fleet as of 9 December 2004 is shown in Table 1. As indicated, four aircraft are active and A20-627 has been retired. Table 1 also describes the usage of each aircraft up to December 2004. In these figures, both full-stop landings and touch-and-go landings are counted as a flight, while full-stop landings count as a full flight cycle, but touch and go landings count as only half a flight cycle.

Table 1 - Status of RAAF B707 fleet.

Aircraft	Total airframe hours	Total flights	Total touch and go landings	Total flight cycles	Status
A20-623	55872.6	23363	7326	19700	Active
A20-624	49855.9	24419	9481	19678.5	Active
A20-627	50234.7	23562	8599	19262.5	Retired
A20-629	59435.7	21537	5616	18729	Active
A20-261	32848.2	22068	4893	19621.5	Active

In the 1990's the United States Air Force (USAF) converted a number ex-commercial B707 aircraft into surveillance aircraft known as J-STARS (Joint Surveillance Target Attack Radar System). The USAF performed a structural risk analysis on the wings of their B707 aircraft to evaluate the effect of Widespread Fatigue Damage (WFD) [1]. That report highlighted lower wing stringers 4, 5, 7 and 8 as high-risk structural details. These stringers on RAAF aircraft are, and have been, managed with inspections specified by Boeing for all B707 cargo aircraft.

In response to the results of the J-STARS risk analysis, the RAAF were concerned about their own aircraft, which had similar numbers of flights and airframe hours to many of the J-STARS. Thus, they tasked the Defence Science and Technology Organisation (DSTO) to perform a risk analysis on the lower wing stringers in RAAF aircraft. This analysis, detailed in Reference 2, used much of the J-STARS risk analysis data as its basis, because at the time there was little data available to describe RAAF B707 usage and condition. This report investigated the use of a variety of inspections to manage the risk of structural failure of the lower wing stringers. It came to the conclusion that external Low Frequency Eddy Current (LFEC) inspection of the stringers was unsuitable for maintaining the risk of failure to the desired level and RAAF decided to implement an inspection program involving High Frequency Eddy Current (HFEC) inspection around the head of each fastener in stringers 4, 5, 7 and 8 from inside the wing. However, the RAAF found that there were two main problems with performing HFEC on stringers 4 and 8 [3]:

- These stringers have a large amount of sealant on them, which must be removed to adequately perform HFEC inspections. This is labour intensive and may cause damage to the stringer.
- There were Occupational Health and Safety concerns, as this inspection requires inspectors to enter the fuel tank.

Because of these problems, the RAAF requested that DSTO review their risk analysis to investigate the possibility that the probability of structural failure may be kept at an acceptable level by performing HFEC inspections on stringers 5 and 7 and LFEC inspections on stringers 4 and 8 [3]. These are the inspection types specified for these stringers by Boeing. The RAAF were also concerned that the DSTO risk analysis had assumed full coverage of stringers 5 and 7, while in reality this inspection is only performed outboard of wing buttock line (WBL) 59.24 [3].

This report details an analysis of the probability of structural failure from fatigue cracking of the lower wing stringer holes common to the wing skin. While making a number of conservative assumptions in order to simplify the analysis, it attempts to show that the risk of structural failure will be kept at an acceptable level while continuing to perform the current Boeing inspections on stringers 4 and 8 and performing internal HFEC around each fastener in stringers 5 and 7 at each Depot Maintenance (DM). It was decided to perform a new risk analysis using data from Bolt Hole Eddy Current (BHEC) inspections of selected fastener holes in stringers 4, 5, 7 and 8 of the RAAF aircraft A20-627 and A20-623. These data, which became available after the original DSTO risk analysis, provide a better indication of the structural condition of RAAF aircraft than the cracks from the teardown associated with the J-STARS risk analysis (which were used in the previous analysis). These data allowed the distribution of crack sizes to be estimated, while the preceding risk analysis performed by the USAF and DSTO provided the other necessary data.

2. Description of critical structure

The main structural elements considered in this analysis are the lower wing stringers 4, 5, 7 and 8. These stringers are in a highly stressed area of the lower wing and are stronger than the other stringers (except stringers 14 and 18, which are equivalent to stringers 4 and 8). Stringers 4 and 8 are known as splicing stringers. In addition to carrying span-wise stress from wing bending, these stringers splice together adjacent wing skin panels that terminate at these stringers. The locations of stringers 4 and 8 are highlighted in Figure 1.

Stringers 5 and 7 are between stringers 4 and 8 and are known as adjacent stringers. The typical geometry of stringers 4, 5, 7 and 8 is shown in Figure 2. The stringers are typically seven inches apart. This geometry was used in the J-STARS risk analysis. Since this analysis uses much of the data from the J-STARS analysis, this geometry is assumed.

The steel fasteners that attach the stringers to the skin typically have a 0.25 in. diameter. There is a single row of fasteners in each of the forward and aft flanges of the adjacent stringers. The fastener spacing for the adjacent stringers and splicing stringers is shown in Figure 3. As shown in this Figure, the splicing stringers have two staggered rows of fasteners on both the forward and aft flanges.

All of the stringers are made of 7075-T6 aluminium alloy. The skins are made of 2024-T351 aluminium alloy between stringer 4 and stringer 8, and 2024-T42 aluminium alloy outside of this panel.

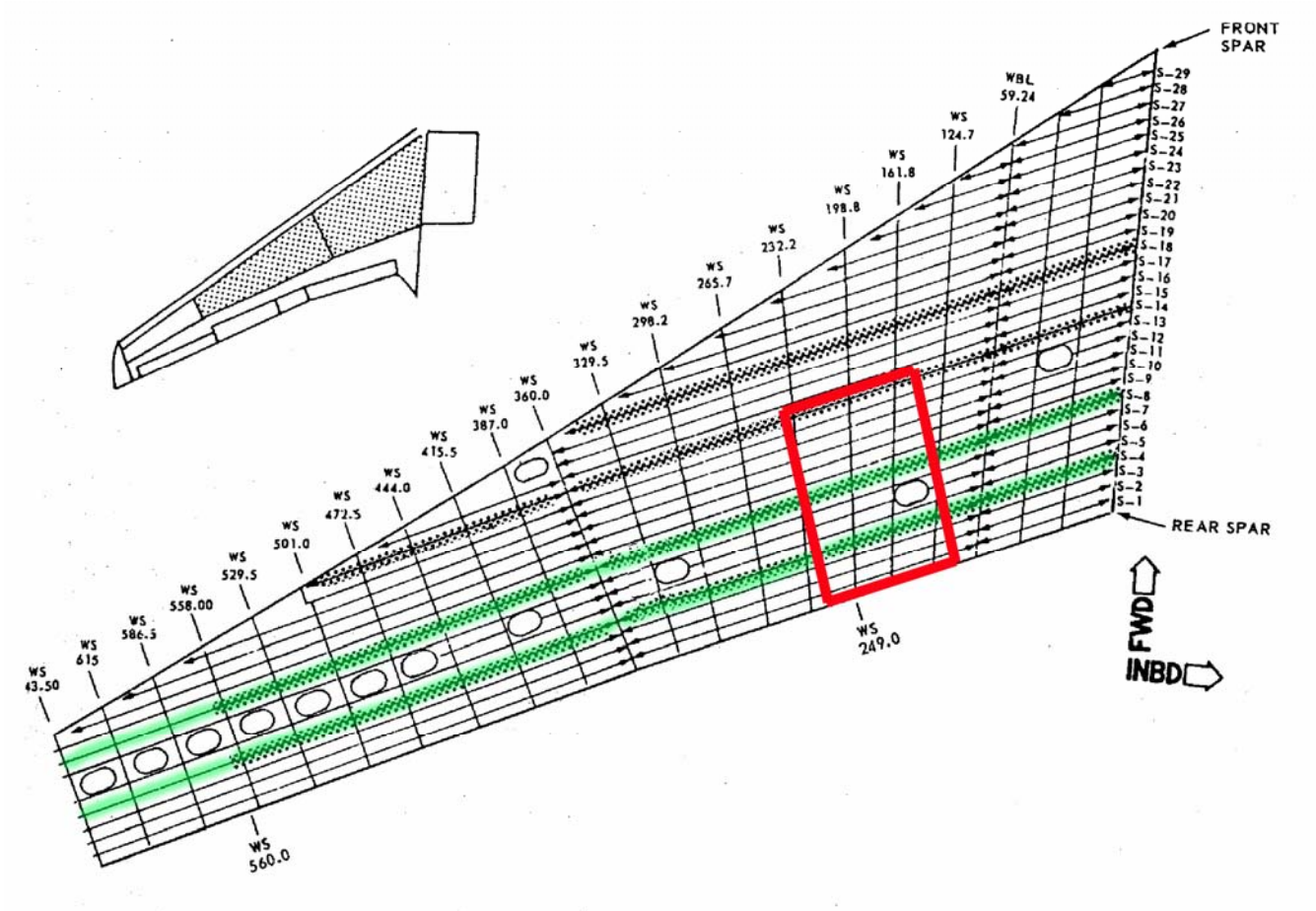

Figure 1 – The B707 lower wing. The locations of stringers 4 and 8 are highlighted in green. The area inspected using BHEC inspection during the B707 LOT study is highlighted in red.

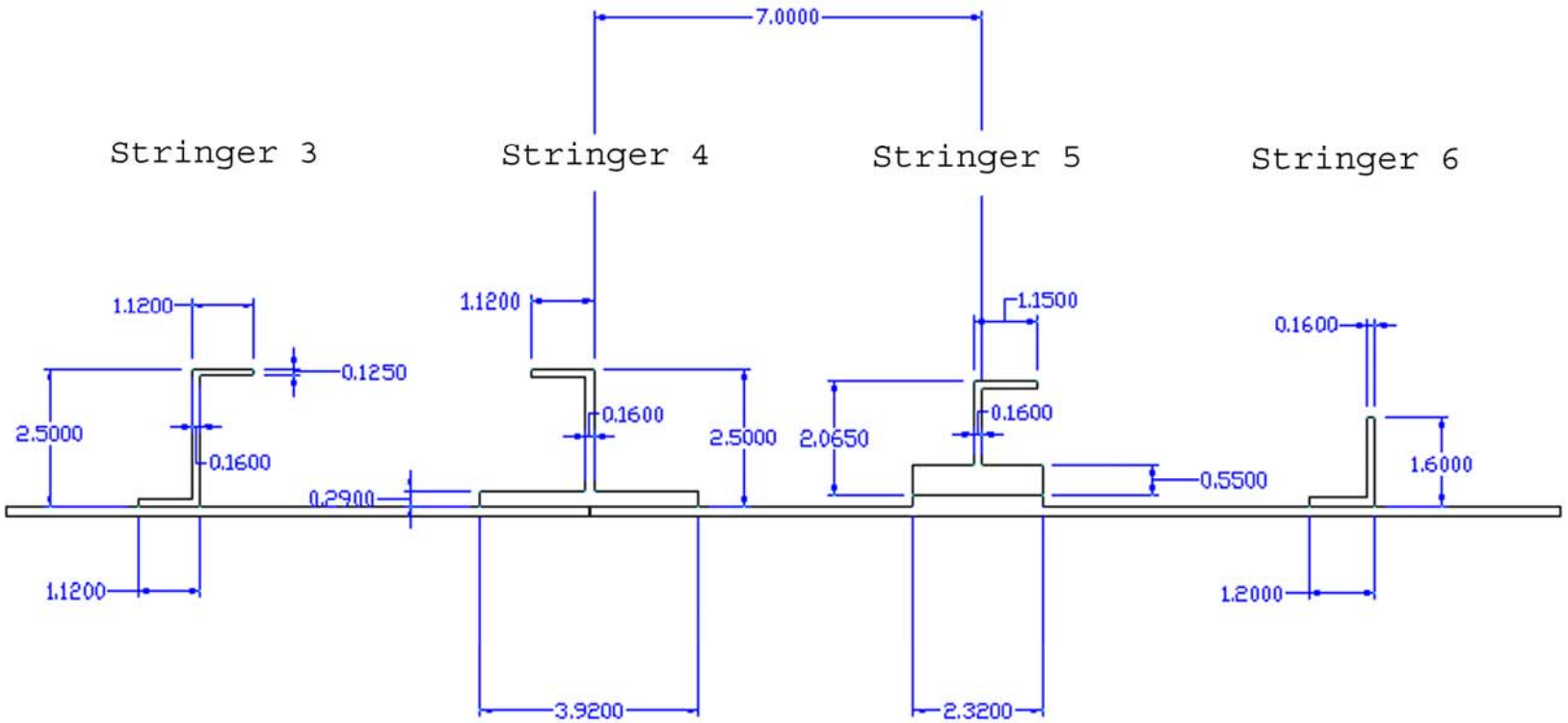

Figure 2 - Typical geometry of the lower wing stringers (dimensions are given in inches).

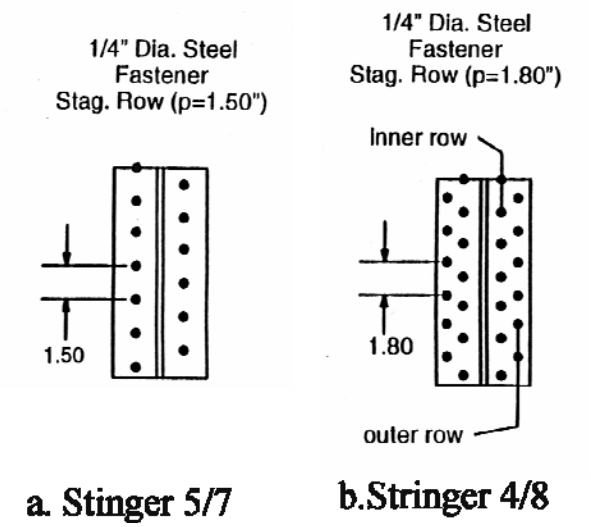

Figure 3 - Typical fastener pitch for lower wing stringers.

3. Inspections

3.1 Boeing inspections

Boeing prescribes the inspection of stringers 5 and 7 in Service Bulletin A3395 [4]. This document calls for HFEC inspection around each fastener attaching stringers 5 and 7 to the wing skins, as well as around the weep holes that allow transmission of fuel through the stringer. The inspection should be done between Wing Buttock Line 59 (WBL 59) and Wing Station 733 (WS 733). The inspection, which should be done every 1300 flights, is done from within the fuel tank and requires removal of excessive or undulating sealant that prevents accurate HFEC reading.

For the stringers 4, 8, 14 and 18, an external LFEC inspection is prescribed as per Service Bulletin 3226 [5]. Reference 4, which also pertains to this inspection, specifies that the LFEC inspection should occur along the full length of the skin gap at the centre of the splicing stringers. The probe location is shown in Figure 4a, which was reproduced from Reference [6]. For the B707-300C the first such inspection should occur after an aircraft has accumulated 17,000 landings and this inspection should be repeated every 1450 landings thereafter [7]. The inspection should take place between Body Buttock Line 70.5 (BBL 70.5) and the outboard nacelle. The outboard nacelle is at a similar location to WS 733, while BBL 70.5 is at the wing root. Thus the main difference between the coverage of the inspections of stringers 5 and 7 and stringers 4 and 8 is the non-inspection between the wing root and WBL 59 for stringers 5 and 7.

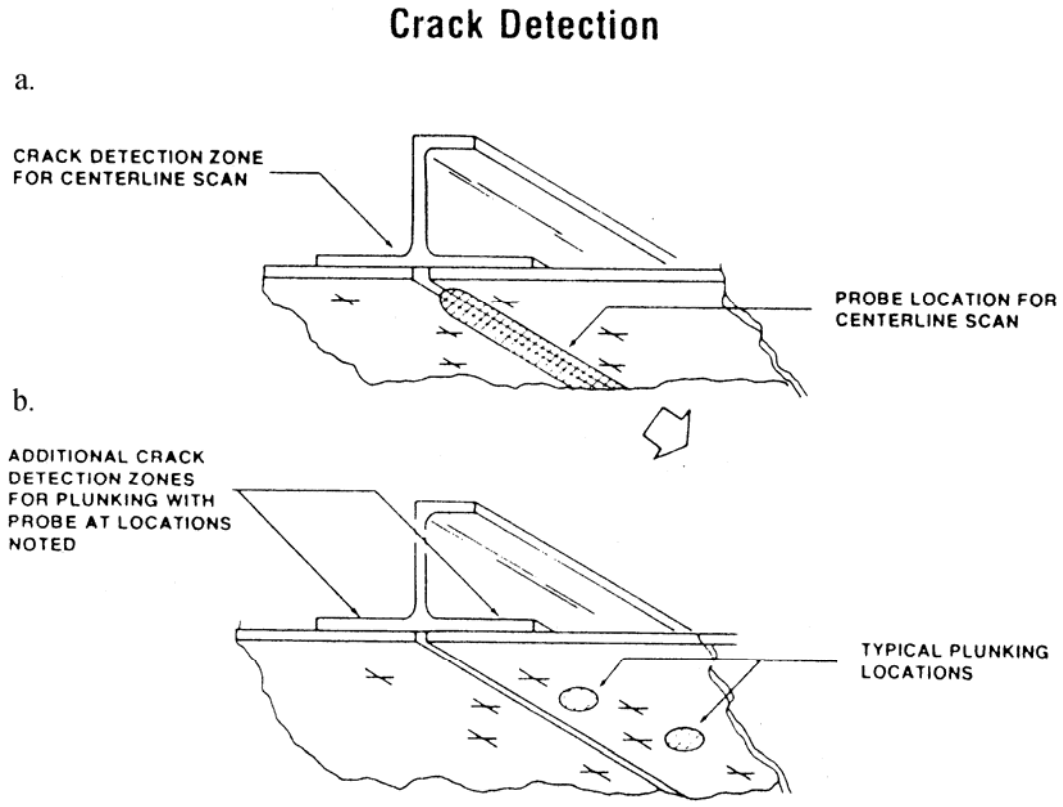

Figure 4 - LFEC inspection on stringers 4, 8, 14 and 18.

3.2 Probability of detection for each method of inspection

For the risk assessment undertaken in Reference 2, DSTO was provided with Probability Of Detection (POD) data related to the inspection of fastener holes between the skin and stringers [8]. In this document, DSTO were given the minimum detectable size (POD=0) and the size of crack that was expected to found 90 percent of the time with 95 percent confidence in this prediction. This figure is commonly known as the 90/95 POD crack length. POD data was provided for three techniques:

1. External LFEC "spotting" at each fastener location. This is presumably similar to the "plunking" given in Figure 4b in addition to scanning the gap between the skins at the splice (see Figure 4a).
2. HFEC around fastener heads.
3. BHEC after removal of fasteners.

The minimum detectable limit and 90/95 POD for each technique are given in Table 2.

DSTO was also advised at this time to treat a POD curve taken from Reference 9 as generic for the eddy current technique and then adjust this curve for the minimum detectability and 90/95 POD limits set out in Table 2.

Table 2 - Probability of detection for cracks growing from fastener holes in the lower wing stringers.

Technique	POD =0 (in.)	90/95 POD (in.)
1. External LFEC	0.500	0.725
2. HFEC around fastener heads	0.250	0.400
3. BHEC after fastener removal	0.010	0.030

3.3 Current RAAF inspections

The RAAF currently inspects stringers 4 and 8 with external LFEC according to Service Bulletin 3226 and SSD 57-A40-05, while stringers 5 and 7 are inspected according to Service Bulletin A3395 as specified by Boeing. The inspection interval given for stringers 4 and 8 is adjusted for RAAF air-to-air refuelling pod usage, while the inspection interval for stringers 5 and 7 is not. The RAAF also perform external LFEC inspection of stringers 4 and 8 at each DM, which is performed approximately every two calendar years on each aircraft. According to the previous risk analysis performed at DSTO, this equates to approximately 900 hours of flying [2].

The current inspection of stringers 4 and 8 is done along the skin gap that is at the centre of the stringer. The detectable crack condition specified for this technique by Boeing is complete cracking of one of the stinger's lower flanges [10]. This is a larger crack size than the 0.725 in. crack that can be found 90% of the time using the spotting technique (specified in Figure 4). Therefore to reduce the risk of these stringers failing, it is recommended that the RAAF alter their inspection of stringers 4 and 8 by adopting this spotting technique adjacent to each fastener (in the chord-wise direction), in addition to the present technique of scanning along the centreline of the flange.

For a short period between approximately 2001 and 2003 the RAAF also adopted HFEC inspection around the head of each fastener on all four critical stringers at each DM.

4. Assumed failure criterion for the wing

The failure condition that was assumed for this risk analysis was based upon information from the J-STARS risk analysis and Boeing analysis. The original J-STARS risk assessment analysed the risk of three failure scenarios [1]:

1. The probability that stringer 7 will fail given that stringer 8 and the skin between stringers 7 and 9 has sustained discrete source damage.
2. The probability that stringer 8 will fail given that stringer 7 and the skin between stringers 6 and 8 has sustained discrete source damage.
3. The probability that either an adjacent stringer or a splicing stringer will fail from fatigue when the remainder of the wing is intact.

The USAF also defined the limits of acceptable risk to be 10^{-3} for Scenarios 1 and 2, while the limit of acceptable risk for Scenario 3 was 10^{-7}. The scenarios and the limits of

acceptable risk reflect that the B707 wing is managed as a fail-safe structure with redundant load paths. The first two scenarios show that the wing can sustain the failure of one of the critical stringers plus two adjacent bays of skin most of the time without failure. Scenarios 1 and 2 calculate the probability that the stringer next to this discrete source damage has sufficient fatigue damage present to fail under the increased loads caused by the failure of the adjacent skin and stringer. These scenarios show that the failure condition for the wing is the failure of two critical stringers that are next to one another plus two bays of skin. The larger than normal limit to the single flight probability of failure (10^{-3}) is a reflection of the fact that the discrete source damage assumed in Scenarios 1 and 2 is very unlikely to occur and could only exist for a short time before being detected.

In Scenario 3, failure of either of the stringers from fatigue is defined as a failure. However, this alone does not cause failure of the wing. It appears that this definition of failure was used in Scenario 3 because the aircraft is certified as a fail-safe aircraft. Thus the wing is no longer fail-safe when one of the critical stringers fails. In this case, according to the certification of the aircraft, it is no longer safe to fly. This definition of failure is obviously conservative in comparison to Scenarios 1 and 2.

The assertion in scenarios 1 and 2 that failure of two critical stringers plus a portion of the skin is required to cause complete failure of the wing, is supported by the Boeing analysis in Reference 10. It defines the critical fail-safe condition as a fully cracked splicing stringer plus a 1.6 in. skin crack below the stringer at this location. It may be assumed that when the splicing stringer is failed, a skin crack that is 1.6 in. long or greater will grow unstably until the nearby adjacent stringer arrests it. This again shows that the failure of two critical stringers next to one another is required for total failure of the wing. A similar critical failure condition would be assumed to exist for adjacent stringers.

In line with the above discussion, the assumed failure condition for the risk analysis was the failure an adjacent stringer and a splicing stringer that are next to one another. The USAF analysis indicated that the failure of two bays of skin around one of the failed stringers is also required to cause complete failure of the wing. Thus it is possible that the wing may still have sufficient strength to prevent failure if the skin in is intact or has minimal cracking, even after the two critical stringers have failed. For the present analysis however, it has been assumed that failure of neighbouring adjacent and splicing stringers alone are required for failure of the wing.

It is also thought that these three element failures (i.e. wing skin, adjacent stringer and splicing stringer) would need to occur at similar span-wise locations for total wing failure to occur. If they occurred at significantly different span-wise locations, then it is quite likely that the wing could still survive by redistributing loads around the failed elements. However, to avoid the added complication of determining how close the element failures need to be to cause total failure of the wing, it has been conservatively assumed that failures anywhere along the spans of the splicing and adjacent stringers are sufficient to cause failure of the wing.

The present analysis does not consider the case of discrete source damage. It is concerned only with degradation of strength due to fatigue damage. Thus for failure to occur, cracks in the skin, an adjacent stringer and a splicing stringer, would need to grow to individual element failure. These failures of the skin and stringers could occur in any order. For example a splicing stringer could fail first, followed by the failure of two bays of the skin, followed by the failure of an adjacent stringer. Another alternative would be that two bays of skin cracked first, followed by an adjacent stringer failure and then by a splicing stringer failure. However, when the skin is the first or second element to fail, it is almost certain it will be found during routine flight line inspections before any further failures occur. This assumption is made because the large size of a two bay skin crack (approximately 14 in.) and the likelihood of fuel leaks as a result of the crack, mean that it is very unlikely that such cracking would be missed in flight line inspections. Thus it is assumed that the cases when the two bays of skin crack before the stringers are not viable failure sequences, and do not contribute to the probability that the wing will fail.

A possible exception, where the failure of the skin could precede the failure of the stringers and then cause failure of the wing, is if one of the stringers fails in the same flight as the skin failure. The scenario would require the skin crack to reach a critical length, plus a nearby stringer crack to also reach a critical length (adjusted for the increase in loads caused by the failure of the adjacent skin if it is in close proximity) in exactly the same flight. The distribution of crack sizes in the adjacent stringers that was derived in Section 8 of this report indicates that in the immediate future it is unlikely that a crack will become critical in a given flight. It is therefore very unlikely that two cracks in adjacent structure (the skin and a stringer) will become critical in the same flight. This scenario is made even less likely by the Life Of Type (LOT) inspection results (see Section 8.1), which indicate that in comparison to stringer cracks, there was a very low incidence of skin cracks, and those cracks that were found were very small [11]. Furthermore, because of the accessibility of skin cracks, their size before they become critical (approximately 1.6 in.) and the possibility of fuel leaks, it is thought that there is a good chance that skin cracks will be found during flight line inspections before a failure of the skin occurs.

Because of the high likelihood that a large skin crack would be found prior to nearby stringers also failing (leading to complete failure of the wing), the case of the wing skin failure occurring before failure of both of the stringers is assumed not to contribute to the overall probability of failure. Thus in the present analysis, the skin is assumed to be intact. This is less conservative than the case the USAF considered in their analysis. However, this is because the present analysis does not include discrete source damage. It is also worth noting that, while the present case is less conservative than Scenarios 1 and 2 in the USAF analysis, the level below which risk must be maintained (see Section 12.2) is also much lower than it was for these scenarios.

In summary then, the assumed extreme condition for wing failure is for stringers 4 and 5, or stringers 7 and 8 to fail from fatigue while the skin is still intact. Considering one pair of adjacent and splicing stringers, the probability of them both failing is:

1. The probability that the splicing stringer fails first, then the adjacent stringer fails. This is the probability that the splicing stringer will fail first multiplied by the

probability that the adjacent stringer will fail given that the splicing has already failed; OR

2. The probability that the adjacent stringer fails first, then the splicing stringer fails. This is the probability that the adjacent stringer will fail first multiplied by the probability that the splicing stringer will fail given that the adjacent stringer has already failed.

In both cases above, an adjacent stringer and a splicing stringer must fail to cause total failure of the wing. In order to simplify the current analysis it was assumed that each splicing stringer in a B707's two wings had failed at a single location. As described by Section 3 of this report, the splicing stringers are regularly inspected and no full break of such a stringer has been found. The assumption of the splicing stringers being failed at the start of the analysis is conservative. In the two cases given above, the probability that the splicing stringer has failed, either first or second, can be at most equal to one. Therefore, assuming a probability of one for the probability that the splicing stringer has already failed at the start of the analysis is conservative. The analysis of such a scenario is also conservative because it assumes that the fatigue damage in the part of the adjacent stringer that is near the splicing stringer failure grows more rapidly due to loads shed from the splicing stringer. It assumes that this condition exists from the start of the analysis. In reality there is only a limited chance that these conditions would occur from the start of the analysis.

The assumption that each splicing stringer had already failed was made because of the low POD of the current LFEC inspections. Reference 10 gives the crack length at the 90/95 POD as the failure of one of the stringer's flanges. Based on the crack growth derived for stringer 7 with RAAF usage (see Section 9), it was thought that if this crack was missed during an inspection, then the stringer may fail before the next inspection (assuming 900 hours between inspections). Unfortunately there was little crack growth data available for stringer 8 in Reference 1. As a result it was difficult to check how long it would take for a cracked through stringer flange to grow until it failed the whole stringer. This lack of crack growth data for stringer 8 was another reason why the simplifying assumption that the splicing stringers had failed in a single location was made.

Finally, it should be noted that the calculations performed in this report are related to the probability of failure contributed by cracking of fastener holes between the flanges of the critical stringers and skin. The teardown inspection of two high time B707 wings that provided crack size data for the J-STARS risk analysis found that most of the cracks in the critical stringers occurred at these fasteners [12]. Other sources of cracking in the stringers have not been considered.

5. Calculation of the probability of failure

The probability that a cracked stringer will fail is the combination of the probability of a structural configuration existing and the probability of experiencing a load big enough to break that structural configuration. In the case of the B707 lower wing stringers, the structural configuration is defined by the cracks present. Assuming that the level of

cracking is independent of the load condition, the conditional probability of a specific cracked stringer failing is the product:

$$\Pr(\textit{failure})_{x=X} = \Pr(x = X) \bullet \Pr(R(x) < S) \qquad \textit{Equation 1}$$

In the above equation, x describes the structural configuration. The function R describes the residual strength (which is a function of x) and S is the load condition experienced.

Given that the residual strength is deterministic, the probability of failure is then a function of the cracking and the load applied. The equation above gives the probability of failure for a single structural configuration and a single load condition. However, many structural configurations may exist in the fleet and the maximum load experienced by an aircraft varies from flight to flight. The aircraft is also more likely to experience some loads than others. Thus to calculate the overall probability of failure, the probabilities of all possible structural configurations and load conditions occurring need to be combined:

$$\Pr(\textit{failure}) = \iint \Pr(x) \bullet \Pr(R(x) < S)\, dx\, dS \qquad \textit{Equation 2}$$

The summation of the probability of failure may be calculated in a number of ways including using Monte Carlo simulations. This is the method used in the present analysis. The Monte Carlo method was applied by simulating the initial configuration and subsequent growth of cracks in an adjacent stringer. At the end of each flight a maximum load condition was simulated and the stringer was tested for failure.

By doing a large number of simulations, the probability of failure can be calculated from the proportion of simulations that have failed at or before the time of interest, t:

$$TPOF(t) = \frac{N_t}{N} \qquad \textit{Equation 3}$$

In this equation N_t is the number of failures at or before t and N is the total number of simulations. The probability of failure calculated in Equation 3, the Total Probability of Failure (TPOF), is the cumulative probability of failure occurring from the starting point of the Monte Carlo simulations. For the present set of simulations, the cracking at the beginning of each simulation was derived from the distribution of crack sizes found during the LOT inspections of aircraft A20-627 and A20-623. Thus by growing the cracks from this point, it is only possible to determine the probability that a stringer has failed after this point, not over the whole life of the aircraft. Thus it is not possible to compare this calculated probability of failure to airworthiness standards that deal with the cumulative probability of failure over the aircraft's entire life. However, another standard measure of probability of failure, the probability that the aircraft will fail in a given flight or Single Flight Probability of Failure (SFPOF) may be derived from the TPOF results that were produced by the Monte Carlo method. This was estimated from the rate at which the TPOF changed per flight.

Sections 6 to 10 describe residual strength, crack growth, largest load per flight and initial cracking information that was derived for use in the Monte Carlo simulations. Section 11 describes a number of Monte Carlo simulations that were used in probability of failure

calculations and Section 12 derives failure probabilities from the Monte Carlo simulation results.

6. Effect on stress of a splicing stringer failure

As detailed previously in Section 4, it was assumed during the present analysis that each of the splicing stringers was broken at a single location. A finite element model of a panel representing a portion of skin and stringers 2 to 10 was built in MSC PATRAN to investigate the effect of a broken splicing stringer. The panel was 70 in. wide (in the chord-wise direction) and 100 in. long (in the span-wise direction). The boundary conditions at one end of the panel simulated a symmetry condition so that the panel was effectively 200 in. long. The geometry of the model was based on that given in Figures 2 and 3. The uniform stress in the panel was achieved by applying a uniform displacement of 0.25 in. at one end of the panel. More specific details of the model are given in Appendix A.

The effect of the splicing stringer breakage was investigated by comparing the stress with and without stringer 4 broken. For the unbroken case, all of the stringers and skin were given boundary conditions to simulate symmetry at one end. To simulate the breakage of stringer 4, these boundary conditions were removed from this end of stringer 4. Figure 5 shows the stress at this end of stringer 5 when stringer 4 is broken. It should be noted that only one stringer is simulated as being broken in the model even though it was assumed each of the splicing stringers are broken at one location. Because the assumption of each splicing stringer being failed is already conservative, it is even more unlikely to have two splicing stringers broken at the same span-wise position where they may influence one another. Thus only one stringer failure was modelled in the span considered.

Figure 6 plots the stress in stringer 5 as a function of the distance from the simulated break in stringer 4, for the case of stringer 4 broken and unbroken. The stress was taken along the fastener line of stringer 5 that is closest to stringer 4. The unbroken result seems to be a little inaccurate at the opposite end to the symmetry plane and the broken case has small undulations in the stress functions at approximately 13.5 in., 40 in. and 67 in. from the symmetry plane. The undulations were caused by a single point on the stringer being fixed in the up-down, forward-aft directions at these locations. The stingers were fixed at these locations to simulate the presence of a rib. In spite of these effects, the model appears to give a general description of the load reduction near the plane of symmetry.

The amount of load increase can be seen in Figure 7, which plots the stress in stringer 5 when stringer 4 is broken, normalised by the stress in the unbroken case. The stress in the unbroken case is close to constant at 26 ksi. When stringer 4 is broken, the stress in stringer 5 is 1.06 times this directly adjacent to the break. It can also be seen from Figure 7, that the stress is at an increased level for only about 17 in. either side of the break.

Because the failure of a splicing stringer only influences the stress in the neighbouring adjacent stringer over a length of 34 in. it was simplest to divide the adjacent stringer into

two sections that could be analysed separately. The two sections were a 34 in. length of adjacent stringer with increased stress due to the failure of a splicing stringer and the remainder of the stringer, which is unaffected by the failure of the splicing stringer. The stresses affecting the 34 in. section of the adjacent stringer near the failed splicing stringer were increased by a factor of 1.06. The modelling of load exceedances and crack growth were adjusted for the stress increase in this region.

The probability of failure for an adjacent stringer was calculated as the combination of the probability of failure of an adjacent stringer near the assumed failure of a splicing stringer plus the probability of failure for the remainder of the adjacent stringer. Separate Monte Carlo simulations were performed to calculate the probability of failure for each section of the stringer. The results were combined by addition by conservatively assuming that the failure probabilities of the two sections were independent.

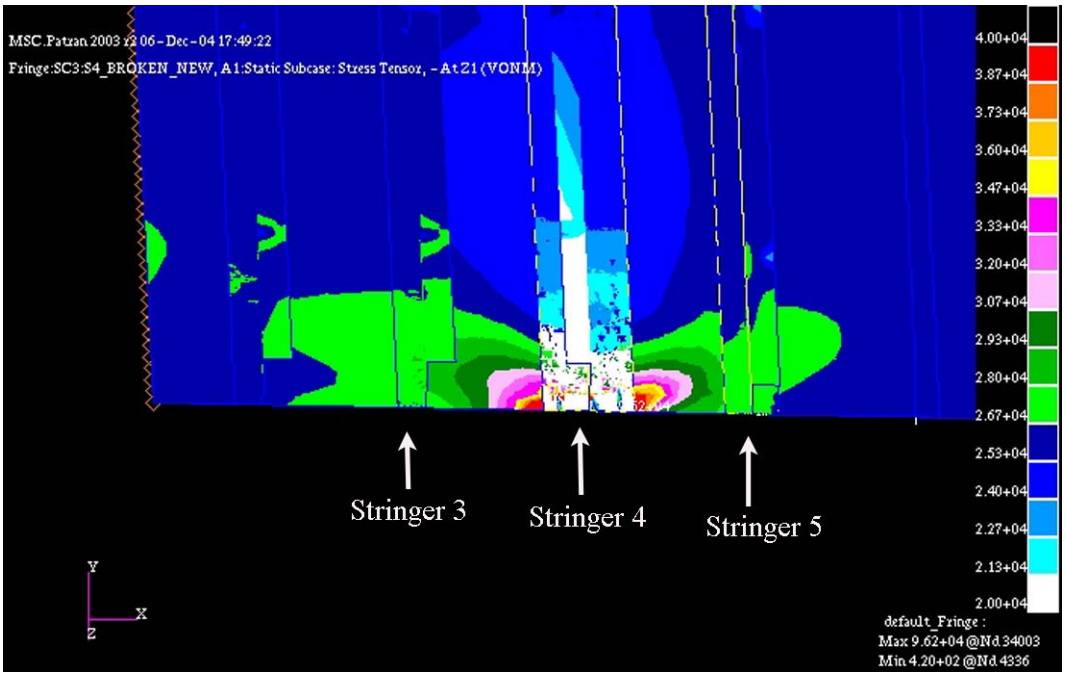

Figure 5 - Finite element model of a B707 lower wing skin panel simulating the breakage of stringer 4.

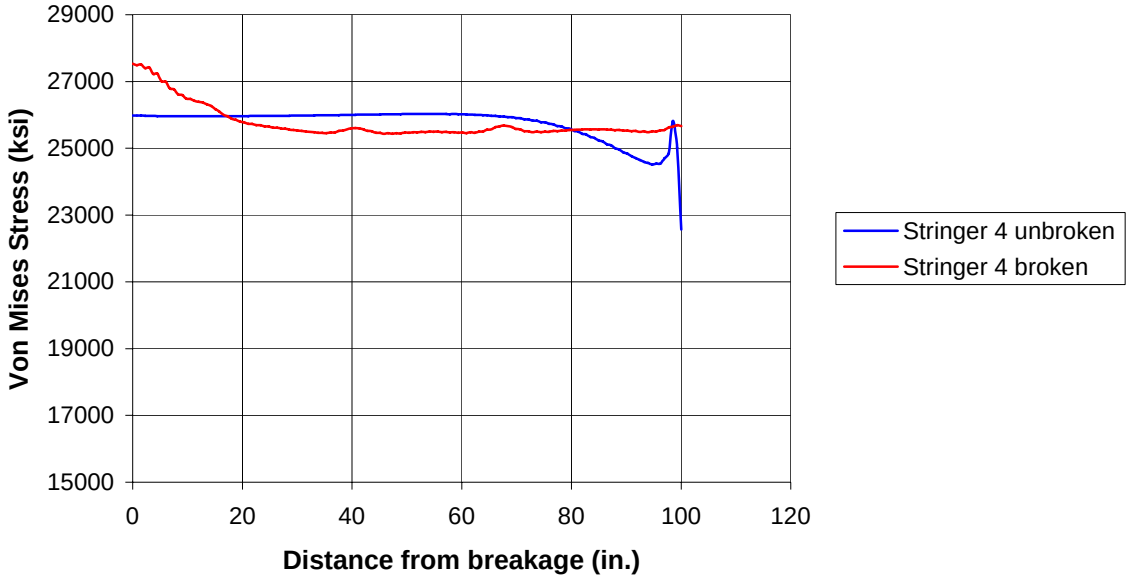

Figure 6 - Stress in stringer 5 as a function of distance from the break in stringer 4.

Figure 7 - Relative increase of stress in stringer 5 adjacent to the break in stringer 4.

7. Probability of load exceedance

The function that was used to describe the probability of the maximum stress experienced in the adjacent stringers in a flight exceeding a certain level was based on the data from the

J-STARS risk analysis [1]. This data gave the probability of the maximum stress in stringer 8 at WS360 exceeding a certain level during a single flight. This data was for the E-8A, an early version of the J-STARS. It was used as a basis primarily because it was the only source available. The missions for this aircraft would not be the same as those for a RAAF B707. However, the largest loads, which are likely to contribute most to the probability of failure, are usually caused by gusts in a transport type aircraft that does not perform any extreme manoeuvres. Thus, this data would adequately describe the RAAF B707 usage if the J-STARS' and RAAF B707's gust environments were similar. This would probably be dependent on the altitude at which missions were flown and weather conditions. However, since one J-STARS flight is on average 9.2 hours long and a RAAF flight is on average 2.76 hours long [2], a J-STARS aircraft will likely see many more gusts per flight. Accordingly, because of the larger sample size, the extreme load per flight is likely to be larger for the J-STARS. Therefore the data from the E-8A is likely to be conservative for RAAF the B707's unless the RAAF B707s fly in a more severe gust environment.

In line with the previous DSTO risk analysis the stress exceedance levels for stringer 8 were scaled by a factor 0.971 to give data for stringer 7 [2]. This factor was given in the J-STARS risk analysis and accounts for the difference in stress levels at the adjacent and splicing stringers [1]. The probability of exceeding a stress in a flight for the splicing and adjacent stringers is shown in Figure 8. This plot also includes the maximum stress in an adjacent stringer when it has been factored by 1.06 to account for the effect of a broken splicing stringer next to it.

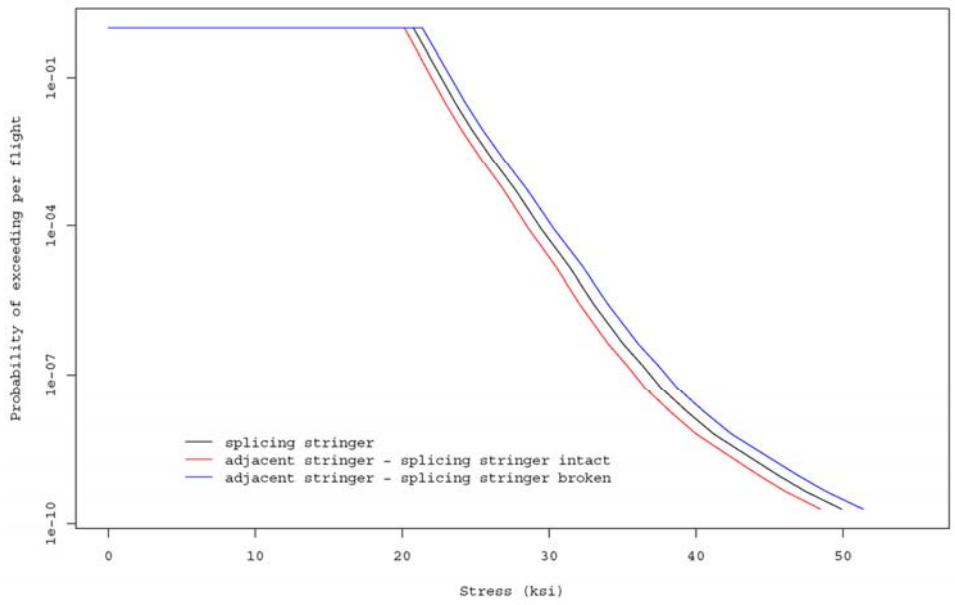

Figure 8 - Probability that a stress level will be exceeded in a single flight.

8. Statistical description of cracks in stringers 5 and 7

8.1 Source of data used in the analysis

The data used for initial crack sizes in this analysis were from the inspection two RAAF B707 aircraft, A20-627 and A20-623, for the B707 LOT study [11]. The details of the usage of each aircraft up to this time are detailed in Table 3.

Table 3 - Usage of aircraft A20-623 and A20-627 up to the LOT inspections.

Aircraft	Maintenance start date	Airframe hours	Touch & go landings	Full stop landings	Flight cycles	Flights
A20-623	May 2000	54697.5	7112	15709	19265	22821
A20-627	Jan 1999	49411.5	8502	14645	18896	23147

The inspection of A20-627 occurred during the 1999 DM on this aircraft. There were two phases of this inspection. The first phase was external LFEC and internal HFEC of stringers 4, 5, 7 and 8 from BBL 70.5 to WS 733. The HFEC involved inspecting around each fastener and along the fore and aft edges of the lower flanges to check if any crack had grown from the fastener hole through to the edge of the stringer. These inspections are described in QANTAS Engineering Document EA SS1929 [11].

The second phase was internal BHEC inspection of selected fastener holes. The area inspected, shown in Figure 1, was chosen to correspond with one of the areas that was inspected to create the data used in the J-STARS lower wing stringer risk analysis [11]. This area covers stringers 4, 5, 7 and 8 between approximately WS 210 and WS 280. According to Reference 11 this area was found to contain the largest cracks and to have the second largest number of cracks during the J-STARS teardown. Reference 11 also details that according to Boeing Stress reports, this area is in the region of highest span-wise stress.

Both wings were inspected for the first phase of inspection, but only the left wing was inspected for phase two, because the right lower skin panel in the area of interest had been replaced in 1993 due to maintenance related damage [11].

There were five positive indications given by the LFEC inspection of the left hand wing, but only one of these indications was confirmed with BHEC inspection. This was a through-thickness crack that ran from a fastener hole to the edge of stringer 4 at approximately WS 553. A number of cracks were found in stringer 4 in the vicinity of this crack. Stringer 5 was checked in this region with BHEC because of the prevalence of cracks in stringer 4. None of the eighteen holes checked gave a positive indication. Inspection with LFEC gave thirteen positive indications on the right hand wing. Six of these indications were confirmed as cracks using BHEC.

The inspection of the wings of A20-623, performed in 2000, had two phases similar to those performed on A20-627. On both wings there were external LFEC and internal HFEC inspections of stringers 4, 5, 7 and 8 completed from BBL 70.5 to WS 733. No defects were found during this inspection. The second phase of inspection, which involved BHEC of open holes, again took place on only the left wing. In addition to the area specified in Figure 1, an inspection of stringer 4, 5, 7 and 8 was undertaken with this method between approximately WS 501 to WS 560. This was probably in response to the large crack found in stringer 4 of the left hand wing of A20-627.

8.2 Results of inspections

The cracks found during the LOT BHEC inspections of A20-627 and A20-623 are described in Tables B1 to B5 in Appendix B. The data from each aircraft were tabulated separately and the data from the splicing stringers and adjacent stringers were also tabulated separately.

From these tables it is possible to determine whether a crack was in the wing skin or a stringer. They also describe the stringer, hole row and approximate wing station of the hole where the crack was found. The fastener hole rows were numbered from forward to aft. The hole rows in the splicing stringers were numbered 1 to 4, while the hole rows in the adjacent stringers were numbered 1 or 2. The "direction" field in the tables describes whether the cracks grew toward the central stiffener in the stringer, or toward the edge of the flange. The type of crack was also described using the abbreviations given in Table B5.

The crack types found in the stringers were:

- Quadrant cracks that grow down the bore of the hole and along the upper or lower surface of the flange. These cracks are designated "edge" cracks in Tables B1 to B5.
- Hole wall cracks that have begun down the hole bore, and have not yet broken through to the upper or lower surface.
- Through-thickness cracks that have grown through the thickness of the stringer flange.

The calculated depth of each crack is listed in Tables B1 to B4. The depth was calculated from the oversize of the hole that was necessary to remove all traces of cracking.

From the data in Appendix B it was possible to make some general comments about the cracking observed:

- Most of the cracks were found in the stringers and not the skin.
- Most of the cracks were quadrant (edge) cracks.
- The largest crack found in either stringer 5 or 7 of both aircraft was 0.206 in. long, while the largest crack found in a splicing stringer had broken through to the outer edge of the stringer (i.e. approximately 0.45 in. long).

8.3 Characterisation of cracking in stringers 5 and 7

The data given in Appendix B were analysed to describe the cracking expected in stringers 5 and 7 of a RAAF B707. A number of aspects of the data needed to be evaluated in order to most accurately predict the cracking in the adjacent stringers. One issue was whether to use the combined data from the splicing stringers and adjacent stringers or just the data from the adjacent stringers. The previous risk analysis conducted at DSTO combined the data from both types of stringers together, while the J-STARS risk analysis characterised the cracking in the adjacent and splicing stringers separately by using crack sizes from the appropriate stringers.

Figures 9 and 10 compare the cracks found in the adjacent and splicing stringers on aircraft A20-627 and A20-623 respectively. In these Figures, the probability of finding a crack within each size interval is given by the height of each column multiplied by the length of the interval. On aircraft A20-627, the cracks in the adjacent stringers were generally smaller, while the cracks from the splicing stringers had a greater variation (see Figure 9). On aircraft A20-623 on the other hand, the cracks in the splicing stringers were very small (see Figure 10). It is not understood why the cracks from the splicing stringers on A20-623 were so much smaller than those from the same stringer on A20-627, especially when the cracks found in the adjacent stringers on both aircraft were similar. Again however, the sizes of cracks in the two different types of stringers appeared to be different.

Table 4 compares the rate of cracking per hole inspected based on the BHEC LOT inspections. The rate is similar for all of the stringers at about 0.10. Again the splicing stringers on A20-627 were the most severely cracked, with about 0.14 cracks per hole inspected.

Although there was no consistent trend between the two aircraft, the crack size data did show significant differences between the cracks in the adjacent stringers and splicing stringers. There are also structural differences between the two sets of stringers (shown in Figure 2), which would imply that cracks in the different stringer types should grow at different rates. This would cause different distributions of crack sizes late in the life of the aircraft. Furthermore, the splicing stringers, as their name suggests, should have additional loads related to splicing adjacent wing skins together. For the reasons outlined above, it was decided that only data from the adjacent stringers would be used to describe cracking in these stringers.

Table 4 - Rate of cracks found during the BHEC inspections.

Stringer	Holes inspected	Cracks found	Ratio of $\frac{cracks\ found}{holes\ inspected}$
A20-627 stringer 5/7	134	14	0.10
A20-627 stringer 4/8	277	39	0.14
A20-623 stringer 5/7	164	19	0.12
A20-623 stringer 4/8	360	33	0.09

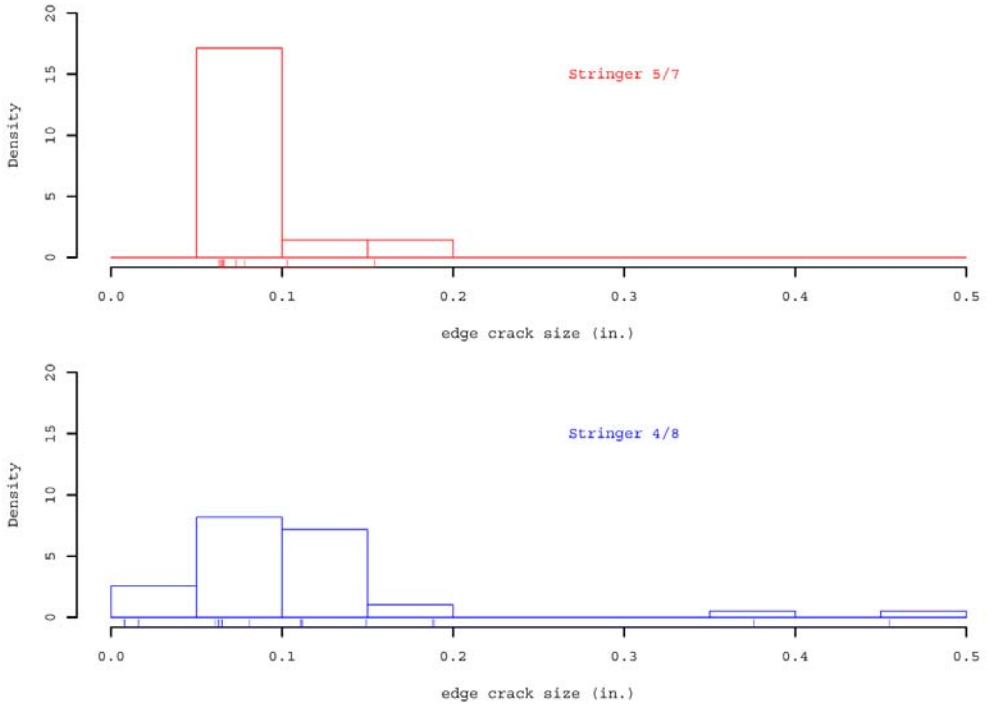

Figure 9 - Histograms of crack sizes in stingers 5/7 and stringers 4/8 found during the BHEC inspection of aircraft A20-627. The ticks on the horizontal axis show the calculated size of each crack.

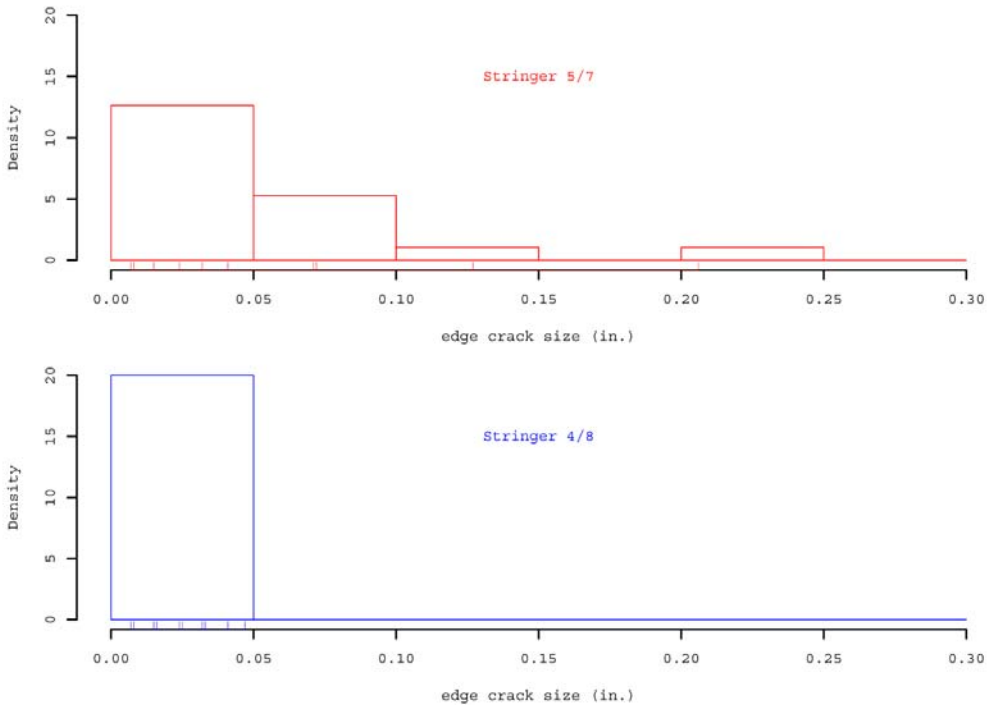

Figure 10 - Histograms of crack sizes in stingers 5/7 and stringers 4/8 found during the BHEC inspection of aircraft A20-623. The ticks on the horizontal axis show the calculated size of each crack.

Another issue that needed to be addressed when fitting a probability distribution to crack size data was the effect of small cracks. As shown in Section 3.2, the 90/95 POD for the BHEC inspection used was 0.03 in. and the predicted smallest detectable crack was 0.01 in. long. This means that for every crack found below the 90/95 POD, many others also below this threshold were missed. The effect of this was that while there wasn't enough small crack data to correctly characterise the whole population, there was still enough to affect a distribution characterising the largest cracks. Since the largest cracks in the stringers contribute most to the risk of failure, it was decided to characterise the larger cracks present by using only cracks greater than the 90/95 POD in the analysis. Because very few of these cracks would have been missed, a probability distribution generated from this data would give a good representation of the larger cracks present.

After removing cracks less than 0.03 in. there were 10 cracks available for analysis from the A20-623 inspection and 14 available from the A20-627 inspection. With so few data points available, it was advantageous to assume that the cracks from both inspections came from the same population, and pool the data. One reason to support this assumption is that at the time of the LOT inspections, both aircraft had flown a similar number of flight cycles and flight hours (see Table 3). Therefore the amount of fatigue should on average be similar if they had flown similar spectra over their lifetimes. The identical structure of the stringers would also support the assumption of similar amounts of fatigue. Finally, since the aim of the present analysis is to estimate the risk of failure for all aircraft in the RAAF B707 fleet, a description of crack sizes for all aircraft, rather than just a single aircraft is most appropriate. Sampling crack sizes from two aircraft will produce a distribution of crack sizes that describes the cracking across the fleet better than data from just a single aircraft.

A histogram of the crack size data from A20-623 and A20-627 is plotted in Figure 11, while Figure 12 gives the normalised cumulative frequency of crack sizes. In both of these Figures, only cracks that were at least 0.03 in. long were plotted. These Figures show lognormal, Weibull and the Generalised Extreme Value (GEV) probability density functions and cumulative distribution functions that were fitted to the data. The data was fitted to two-parameter lognormal and Weibull distributions, which assume the data is greater than zero. In the present case, since only crack sizes greater than 0.03 in. were used, the data were first transformed by subtracting 0.03 in. from each data point to better fit the two parameter distributions (the 0.03 in. was added back on to the crack sizes when they were used in the analysis).

The lognormal distribution has a probability density function of the form [14]:

$$f(x) = \frac{1}{sx\sqrt{2\pi}} \exp\left(-\frac{(\ln(x) - m)^2}{2s^2}\right) \qquad \textit{Equation 4}$$

where m and s are the mean and standard deviation of the data when the natural logarithm of each data point has been taken. Thus the data could be approximated by a lognormal distribution by taking the natural logarithm of each crack size and then

calculating the mean and standard deviation of this transformed data. The lognormal distribution characterising the crack sizes was hence defined by the following parameters: m = -3.307 ; s = 0.860

The data was also described by a Weibull and a GEV distribution. The two-parameter Weibull probability density function has the form [14]:

$$f(x) = \frac{\beta}{\delta}\left(\frac{x}{\delta}\right)^{\beta-1} \exp\left[-\left(\frac{x}{\delta}\right)^{\beta}\right] \qquad \textit{Equation 5}$$

where β, the shape parameter and δ, the scale parameter must be greater than zero.

Also, the GEV distribution is described by a probability density function of the form [15]:

$$f(x) = \exp\left\{-\left[1+\frac{\xi(x-\mu)}{\theta}\right]^{-\frac{1}{\xi}}\right\} \qquad \textit{Equation 6}$$

where μ, θ and ξ are the location, scale and shape parameter respectively and θ must be greater than zero.

The parameters β, δ, μ, θ, ξ for the Weibull and GEV distributions that best described the crack size data were estimated using the maximum likelihood method [14].

The values of β = 1.43 and δ =0.053 describe the Weibull distribution that best fits the distribution of crack sizes larger than 0.03 in. in stringers 5 and 7.

The values of μ = 0.032, θ = 0.021 and ξ = 0.13 describe the GEV distribution that best fits the distribution of crack sizes larger than 0.03 in. in stringers 5 and 7.

From Figures 11 and 12 it can be seen, that all of the distributions investigated gave reasonable, but not excellent fits to the inspection data. It was decided to use the lognormal distribution to describe the distribution of crack sizes because it gave the most conservative predictions. This can be seen when comparing the expected largest crack in an adjacent stringer predicted by each distribution. Given that the cumulative probability distribution function $F(x)$ describes the probability that a crack at a hole will be smaller than x, the probability that the largest of n cracks exceeds x is $1-F^n(x)$ [16]. Using this relationship, it was possible to estimate the average largest expected crack in an adjacent stringer for each distribution fit to the inspection data. The number of cracks, n, was estimated from the expected number of cracks larger than 0.03 in. in an adjacent stringer.

During the LOT inspections of the left wings of A20-623 and A20-627 a total of 298 holes in stringers 5 and 7 were inspected using BHEC inspection and 24 cracks larger than 0.03 in. were found. This gives a rate of 0.081 cracks, larger than 0.03 in., found for every hole inspected. According to the previous DSTO risk analysis, there are 1200 fastener holes in stringers 5 or 7 that attach to the skin below [2]. Based on the rate of cracks found during

the LOT inspections, it is estimated that there will be on average 97 cracks larger than 0.03 in. in each of the adjacent stringers.

Assuming there are 97 cracks in each adjacent stringer, the average largest crack expected in an adjacent stringer based on the lognormal, Weibull and GEV distributions that were fitted to the inspection data were 0.33 in., 0.19 in. and 0.21 in. respectively. The cumulative probability that the largest crack in an adjacent stringer is less than x, given by the lognormal, Weibull and GEV distributions, are shown in Figure 13.

As detailed in Tables B1 to B4, the largest crack found in stringers 5 or 7 during the LOT inspections of A20-623 and A20-627 was 0.206 in. Given that HFEC was performed around each fastener hole of stringers 5 and 7 on both aircraft at the LOT inspections and no crack as big as the average largest crack predicted by the assumed lognormal distribution has been found, it would appear that the lognormal distribution is a conservative description of the cracks present in RAAF aircraft. The 90/95 POD supplied for this HFEC technique is 0.4 in., so some cracks around 0.3 in. long may have been missed during inspection. However on the evidence available it seems that the cracks present are smaller than the largest cracks predicted by the lognormal distribution used to describe crack sizes in this analysis. Furthermore, since the cracks used to derive the lognormal distribution were sampled from the region that was predicted to have the largest cracks (according to the results of the J-STARS teardown) and the highest stress (see Section 8.1), then it is likely that this distribution is conservative for the remainder of the stringer.

Finally, standard HFEC inspections in accordance with Service Bulletin A3395 of all RAAF B707s over approximately the last eight years have not found any cracks as large as 0.33 in. [17]. In fact, the only cracks found at fastener holes between the stringers and skins in this time period were 0.25 in. and 0.08 in. long respectively. Both of these cracks were found on aircraft A20-624 [18]. Given that repeated inspections have not found cracks as large as the largest expected according to the assumed lognormal crack size distribution, this distribution is probably conservative. Furthermore the extreme cases that might be predicted for the worst aircraft in a large fleet of aircraft where the largest cracks in stringers are much larger than 0.33 in. (the predicted average largest crack per wing) do not seem to be present in the RAAF fleet. Thus the evidence gained from inspections would indicate that probability of failure estimates made using the lognormal distribution estimate for crack sizes will be conservative for the RAAF fleet.

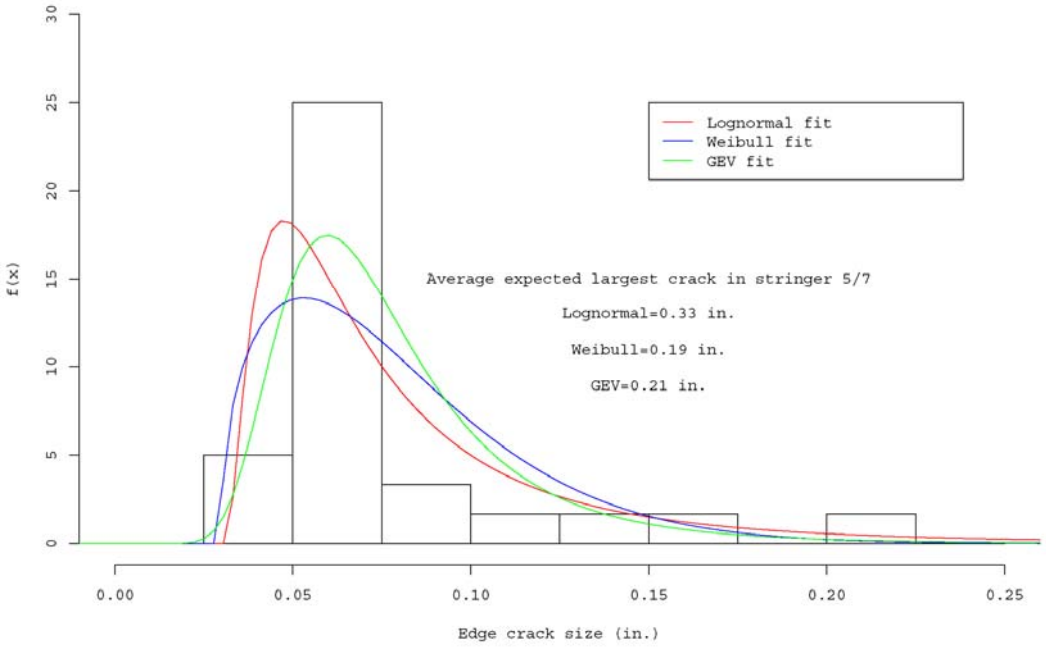

Figure 11 - Histogram and probability distribution function fits of A20-623 and A20-627 crack lengths.

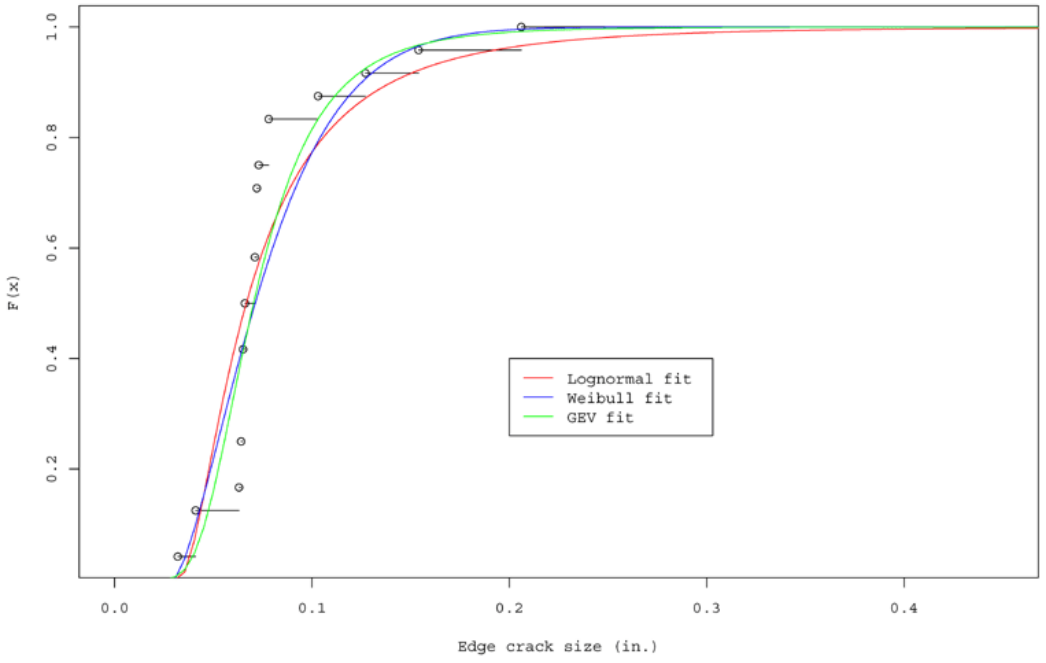

Figure 12 – Normalised cumulative frequency and probability distribution function fits of A20-623 and A20-627 crack lengths.

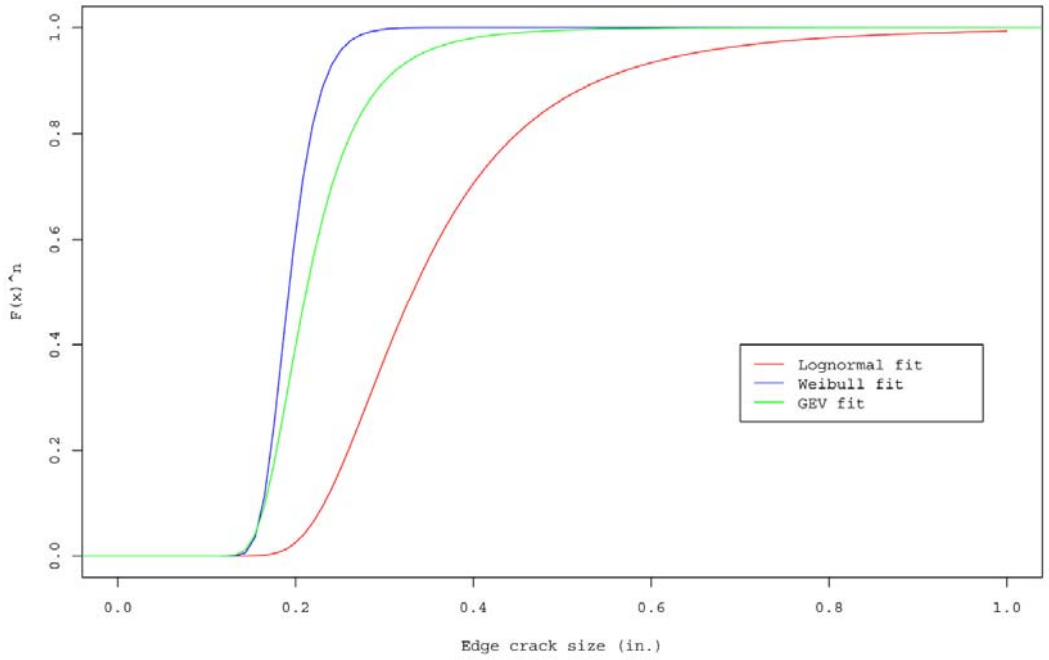

Figure 13 - Cumulative probability that the largest crack in an adjacent stringer is less than x.

9. Estimation of the rate of crack growth

The basis of the estimated rate of crack growth was a crack growth curve derived for stringer 7 of the E-8C J-STARS in Reference 1. This curve was for a single corner crack growing from a filled skin/stringer hole with a 0.25 in. diameter. The curve was derived for 7075-T6 aluminium alloy and it used the Wheeler model of crack growth retardation with an empirical exponent of 0.8.

The crack growth curve that was derived for the J-STARS analysis assumed a single corner crack that grew from a hole out to the edge of the stringer, then back towards the central stiffener [2]. In the present analysis it has been assumed that there are initially two cracks at the critical hole, one growing toward the edge of the stringer and the other growing toward the central stiffener. This assumption was made because the crack data collected during the LOT inspections indicated that while on most occasions cracks were on only one side of holes, there were some holes with cracks on both sides. Thus the assumption of a single corner crack may not be conservative on some occasions.

To allow the use of the USAF crack growth curve, the two edge cracks were approximated as a single corner crack growing to the edge of the stringer. The length of this crack was the sum of the two crack lengths assumed on either side of the hole. The sum length of the edge cracks plus the hole diameter (a common measure of the crack length for cracks growing from holes) is the same in both cases. However the assumption is conservative, because the position of the crack tip has been moved closer to the stringer edge, which would increase the predicted rate of crack growth. Also, the depth of a single large corner

crack through the stringer thickness is greater than the depth of either of the individual cracks it approximates.

The above assumption allowed the use of the curve from the J-STARS analysis, but it was also necessary to adjust crack growth for RAAF usage. The first step of this adjustment was to scale the crack growth from J-STARS usage to commercial cargo usage. According to Reference 2, commercial cargo usage is 1.47 times as severe per flight hour as the E-8C J-STARS aircraft. Thus the life to any crack length given by the E-8C J-STARS curve was divided by 1.47.

The next step of the adjustment was to scale the crack growth to allow for the difference between commercial cargo usage and RAAF usage. The Relative Crack Growth (RCG) per thousand hours for RAAF usage in the period between July 1998 and December 2001 was compared to that of the commercial cargo aircraft (both detailed in Reference 19). Using the average RCG for the RAAF aircraft, it was calculated that RAAF usage per hour was 1.14 times more severe than that of a commercial cargo aircraft. Accordingly, the life to any crack length given by the commercial cargo crack growth curve was divided by 1.14. Figure 14 shows the original J-STARS crack growth curve as well as the commercial cargo and RAAF curve that were produced by factoring the rate of crack growth.

Finally, an estimate of the increase in crack growth was made for cracks near a break in a splicing stringer. Using the increase in stress estimated in Section 6, it was assumed that all the tensile stresses experienced at the crack increase by a factor of 1.06 when there is a splicing stringer failure nearby. It is possible to estimate the change in crack growth life when the stress spectrum has been scaled with the formula [20]:

$$L_2 = \left(\frac{\Delta\sigma_1}{\Delta\sigma_2} \right)^n L_1 \qquad \textit{Equation 7}$$

In this formula, L_1 is the life at the original stress range, $\Delta\sigma_1$, L_2 is the life at the factored stress range, $\Delta\sigma_2$, and n is a material exponent. In the case of 7075-T6 aluminium alloy, n is equal to 3.21. Thus the effect of a factor of 1.06 on the stress range is:

$$L_2 = \left(\frac{1}{1.06} \right)^{3.21} L_1 = 0.83\, L_1 \qquad \textit{Equation 8}$$

The crack growth curve that was produced when this factor was applied to the RAAF usage curve is also shown in Figure 14.

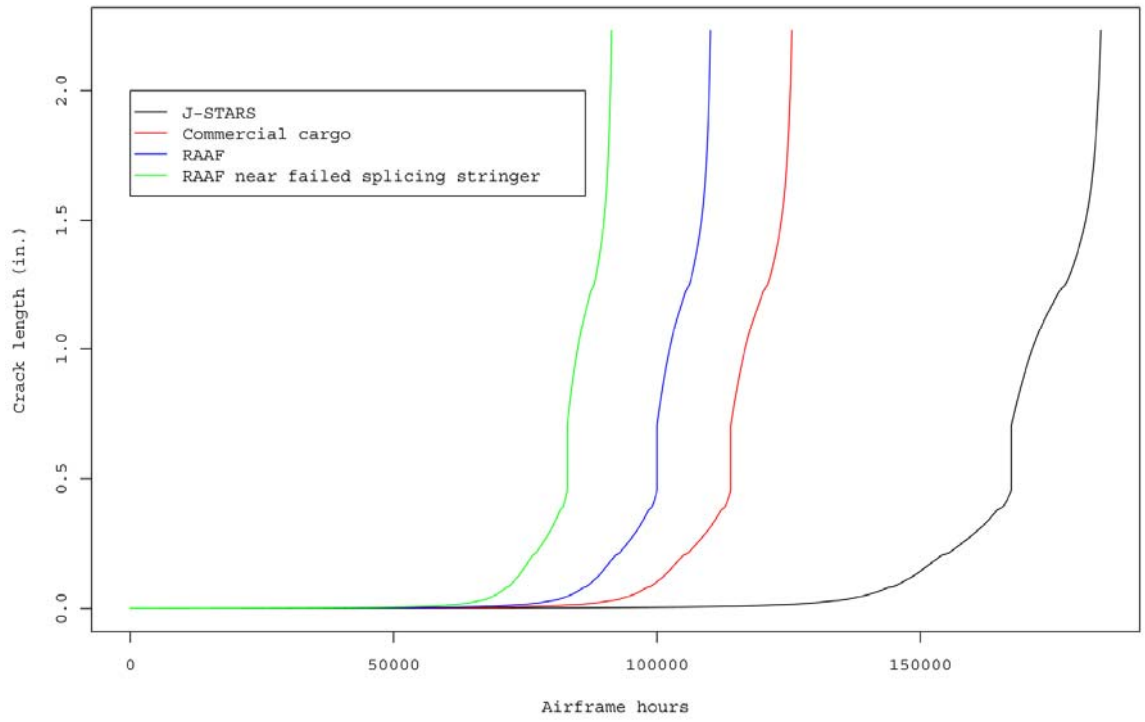

Figure 14 - Stringer 7 crack growth curve for E-8C J-STARS, commercial cargo and RAAF usage.

10. Estimation of the residual strength of adjacent stringers

The residual strength model used in this analysis was taken from the J-STARS analysis in Reference 1. This curve was produced under the assumption of a single corner crack growing from a hole to the edge of the stringer and then back towards the central stiffener (the same assumed case as for crack growth in the J-STARS risk analysis). The residual strength was given as the stress causing failure as a function of crack length (see Figure 15). As was the case for the estimation of crack growth, the two cracks that were assumed to be present at the critical fastener hole were approximated by a single crack that was the sum length of these two cracks. This approximation was conservative for the same reasons that the approximation used for crack growth was.

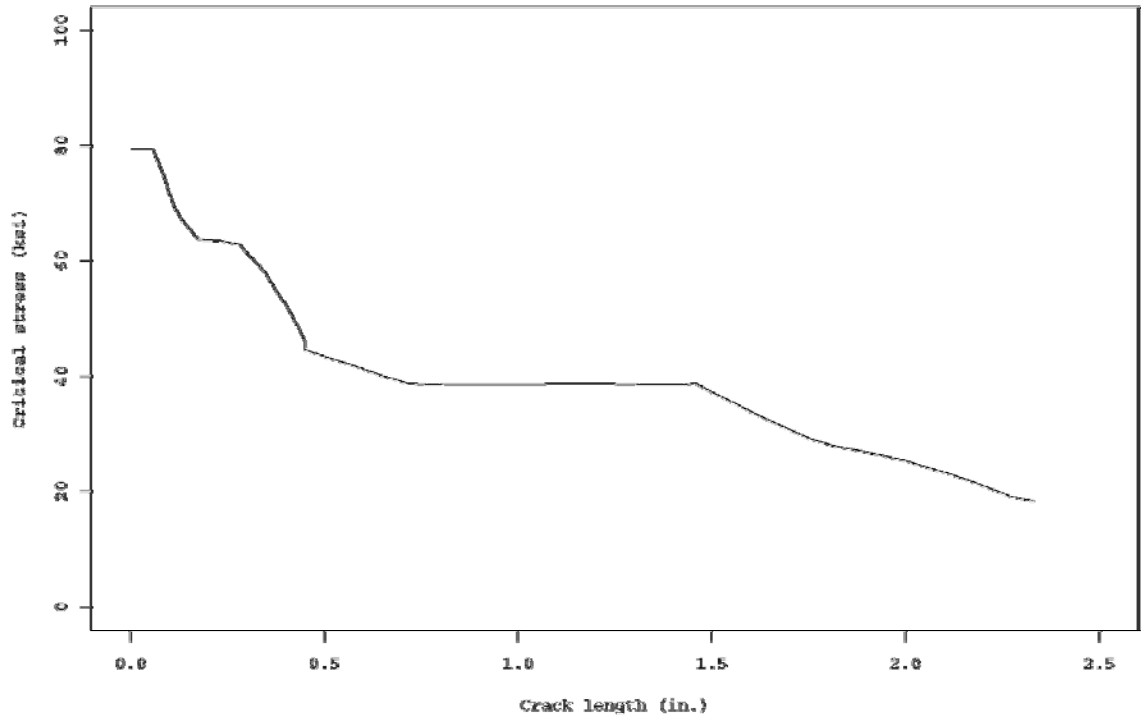

Figure 15 - Stress required to fail stringer 7 as a function of crack length.

11. Description of Monte Carlo simulations

A number of sets of Monte Carlo simulations were performed to calculate the probability of failure for various portions of the wing under different conditions. Separate simulations were performed for the section of the adjacent stringer that was affected by the failure of the nearby splicing stringer and for the remainder of the stringer. A separate simulation was also performed for the portion of the stringer inboard of WBL 59.24, where no inspections are possible. Finally, simulations were also performed on the stringer with and without inspections to evaluate the affect that inspections have.

The remainder of this section describes the simulations that were performed, while Section 12 describes the results and combines a number of them to make an estimate of the probability of failure for RAAF B707 wings.

11.1 Simulations without inspections

The probability of failure was first calculated assuming that no inspections were conducted. The total probability of failure for a single adjacent stringer was estimated using two separate sets of simulations. The first set of simulations was for cracks in the 34 in. section of stringer adjacent to the assumed failure of a splicing stringer. The other set of simulations was for the remainder of the stringer. It was assumed that from the start of

the analysis there was a break in each splicing stringer. The finite element analysis in Section 6 showed that the area of a stringer neighbouring this break in the splicing stringer experienced more severe stress, which affects both the rate at which cracks grow and the most severe loads this section of stringer needs to withstand. To accurately model the growth of cracks in all of the stringer, it was decided to model the region neighbouring the failure of a splicing stringer separately to the remainder of the stringer.

The result of each simulation was the time of failure. In each stringer section of interest, only the fastener hole with the largest cracks was considered. This was done since (given that stress is essentially constant along the span of the stringers) all of the cracks are affected by the same loading mechanism, meaning that the largest crack will always fail first and thus contributes all of the probability of failure. Since it was assumed that there were no inspections for this set of simulations, there was no possibility of the largest crack being found and repaired, so this hole was critical throughout the simulation.

There was also a set of simulations done for cracks present in the 59.24 in. of the stringer that is not inspectable (inboard of WBL 59.24).

11.1.1 Simulations for the section of stringer adjacent to the failure of a splicing stringer.

The starting point of this simulation was an estimation of the number of cracks present in this 34 in. span of stinger. Based on the typical geometry of an adjacent stringer, shown in Figure 3, there is a fastener every 0.75 in. along the stringer. Based on this spacing, one would expect approximately 45 holes in a 34 in. length of stringer. Given that the LOT inspections found about 0.081 cracks (> 0.03 in.) per hole inspected, it would be expected that there would be 4 cracks in a 34 in. span. Thus 4 cracks were randomly chosen from the lognormal distribution of crack sizes defined in Section 8.3. To account for the fact that 0.03 in. was subtracted from each crack size when the lognormal distribution was derived, 0.03 in. was added on to each of the four crack sizes generated before the simulation proceeded.

It was assumed for the simulation of cracking in this highly stressed region adjacent to the failure of a splicing stringer, that the two largest of the four expected cracks were located at either side of one fastener hole. The remainder of the simulation was performed for this pair of cracks at a fastener hole. The larger of the two cracks was assumed to be closest to the edge of the stringer. If it was larger than the edge distance from the hole to the edge of the stringer, then its length was assumed to be this edge distance. In this case, the total crack length would be the edge distance plus the hole diameter and the crack on the other side of the hole.

At this stage of the simulation, the residual strength of the stringer was calculated for the cracks present and a maximum flight stress was randomly chosen from the distribution of the maximum load levels for the region of stringer adjacent to the failure of a splicing stringer (defined in Section 7). If the maximum load exceeded the residual strength then the stringer was assumed to fail.

From this point onwards, the cracks at the fastener hole were grown according to the crack growth curve defined for the highly stressed region of the stringer (see Section 9) in blocks of 50 hours. The interval of 50 hours was chosen arbitrarily, while attempting to reduce the overall time of simulations and to keep the interval small enough to minimise interpolation when making predictions from the results. Because a deterministic crack growth curve was used, the accuracy of crack growth predictions was not affected by the size of the interval. At the end of each block, failure was tested according to the comparison of the residual strength of the stringer with the largest of loads randomly generated for 50 hours of flying.

11.1.2 Simulations for the remainder of the adjacent stringers.

The starting point for this set of simulations was to estimate the worst case of cracking present in the stringers outside of the region that was adjacent to the failure of a splicing stringer. As detailed in Section 8, from the rate of cracks found during the LOT inspections, it was expected that there would be 97 cracks greater than 0.03 in. present in each adjacent stringer. Given that in the previous paragraphs it was estimated that one could expect 4 cracks in the span of stringer adjacent to the failure of a splicing stringer, there should be 93 cracks of interest in the remainder of the stringer.

The starting point of the simulation was to randomly generate 93 cracks from the lognormal distribution used to describe cracking in the adjacent stringers. Again, to account for the transformation of the crack size data that was performed before the lognormal distribution was generated (i.e. minus 0.03 in.), 0.03in. was added to each crack size that was selected from the distribution. The largest of these cracks was then chosen to be on the stringer edge side of the critical fastener hole. If this crack's length exceeded the edge distance, then it was set to be equal to the edge distance. The crack on the other side of the hole was then chosen as any other crack from the 92 remaining cracks.

It was hypothesised that the crack on the opposite side of a fastener hole with the largest crack in the stringer, may be larger than average due to the stress conditions caused by the presence of the large crack. However, comparison of the cracks found during the LOT inspections at either side of holes showed little correlation between the sizes of the cracks. This comparison, illustrated in Figure 16, indicated that in most cases there was a significant crack (i.e. >0.03 in.) only on one side of the hole. There were six holes where the crack size data indicated that the size of cracking was identical on both sides of the holes. However, this was a consequence of the length of both cracks being estimated from the oversize of hole necessary to remove the largest crack at the hole. Even with this biased data considered, it can be clearly seen from Figure 16 that cracks on one side of the hole do not necessarily cause cracks on the other side. Thus it was decided that it was acceptable to combine the largest crack in the stringer with any other that might be found in the stringer. The assumption of cracks on both sides of the holes may in some cases be conservative, as the data appears to suggest that for the majority of holes, cracks are present on only one side of the hole.

Similar to the case of the 34 in. span adjacent to the failure of a splicing stringer failure (detailed above), the assumed critical cracking condition was checked to see if it would fail

in its initial condition. After this initial check, the critical cracks were grown according to the crack growth curve given in Section 9 in blocks of 50 hours. At the end of each 50 hour block the stringer was checked to see if the stringer had experienced a load that exceeded its residual strength in the last 50 hours, assuming the crack lengths at the end of the 50 hour block.

11.1.3 Simulations for the region of stringer inboard of WBL 59.24.

The RAAF advised that the section of adjacent stringers inboard of WBL 59.24 could not be inspected [3]. Thus a separate set of simulations were conducted for this region. As detailed above, the typical geometry of an adjacent stringer indicates that there is a fastener hole every 0.75 in. Thus in a span of 59.24 in. one would expect about 79 fastener holes. Given that the LOT inspections found about 0.081 cracks (>0.03 in.) per hole inspected, it would be expected that there would be 6 cracks in a 59.24 in. span.

Six cracks were randomly chosen from the lognormal distribution describing cracks sizes in the adjacent stringers to represent the six expected cracks in the region of a stringer inboard of WBL 59.24. Again, to account for the transformation of the crack size data that was performed before the lognormal distribution was generated (i.e. minus 0.03 in.), 0.03in. was added to each crack size that was selected from the distribution. It was assumed that the largest of these six cracks was on the stringer edge side of the critical fastener hole in this region. As for the simulations detailed above, the length of this crack was limited to the edge distance from the hole to the edge of the stringer. One of the remaining five cracks was randomly chosen to be present at the other side of the critical hole. The cracks at this hole were grown according to the crack growth curve defined in Section 9 in blocks of 50 hours. At the end of each 50 hour block, the stringer was checked to see it had experienced a load that exceeded its residual strength in the last 50 hours. The residual strength in these checks was based on the crack length at the end of the 50 hour block.

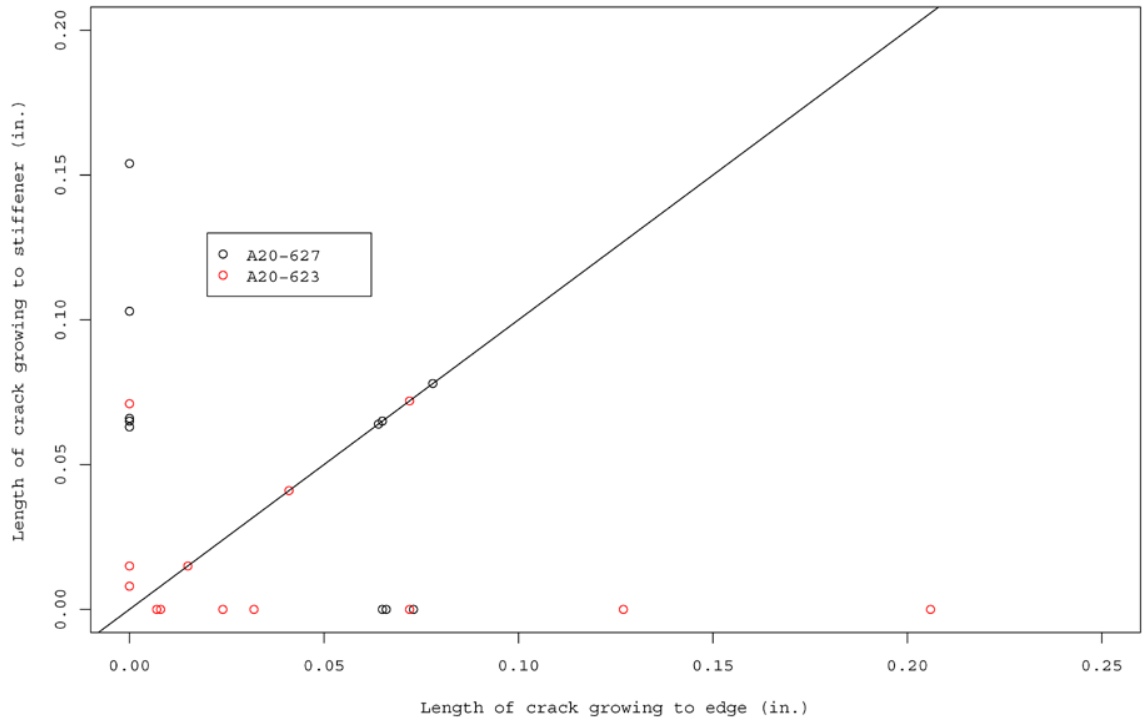

Figure 16 - Comparison of the length of crack growing towards the edge of the stringer on one side and towards the central stiffener on the other side at each cracked fastener hole. The straight line shown indicates there are cracks of identical length on both sides of the hole.

11.2 Simulations with inspections

Simulations were also performed assuming inspections around each fastener hole with HFEC at the start of the simulation period and every 900 hours afterwards. This interval of 900 hours between inspections was chosen, because according to Reference 2 the aircraft may be inspected every two years at their scheduled DM, which is equivalent to 900 hours flying. The HFEC inspections were simulated for each crack with a binomial trial that had the following probabilities of success (i.e. POD):

1. For cracks bellow the 90/95 POD (0.4 in.) it was assumed that the POD was 0.
2. For cracks at or above the 90/95 POD the POD was assumed to be 0.90.

The 90/95 POD only was used rather than the whole POD curve that was derived in the previous DSTO risk analysis of the stringers [2], because this derivation assumed a generic POD curve shape for the eddy current method. However, in reality the POD of any inspection is specific for that inspection because of details such as access, obstructing fastener heads and the orientation of cracks. Thus adjusting a generic POD may be inaccurate and unconservative. For this reason, it was decided to use the data that was specifically derived for the HFEC inspection used, which was the 90/95 POD. By using this single point the simulated inspections are likely to give a conservative estimate of the cracks found during an inspection.

It was assumed that cracks that were found during inspection were removed completely when repaired. This assumption was made because the cracks already present in the stringers are the result of approximately 19,000 flight cycles (see Table 1), so even with poor repair quality, cracks that have been found and repaired would be expected to be much smaller than those present since early in the aircraft's life. For this reason repaired cracks would make little contribution to the overall probability of failure and thus removing them from the simulation will make little difference to the end result.

As detailed above for the case of no inspections, 4 cracks were generated to represent the damage in the section of stringer adjacent to the assumed failure of a splicing stringer and 93 cracks were generated to represent the damage expected in the remainder of the stringer. In all cases, 0.03 in. was added to the crack sizes that were selected from the distribution to adjust for the subtraction of 0.03 in. from the crack sizes that were used to generate the lognormal distribution. For the simulation of the region adjacent to the failure of a splicing stringer, the four cracks were assumed to be at two critical fastener holes. The largest two cracks were on the side of the holes closest to the edge of the stringer and the other two cracks were on the other side.

For the case of the section of stringer not adjacent to a splicing stringer failure, 92 cracks were modelled, with a crack on either side of 46 holes. The 46 largest cracks were assumed to be on the side of the hole closest to the edge of the stringer. The remaining 46 cracks were randomly located on the other sides of the holes. As detailed above, there did not appear to be correlation between the sizes of cracks on opposite sides so it appeared reasonable to randomly pair cracks. It may be argued that by separating the 46 largest cracks, one reduces the chances of seeing large cracks on either side of one hole. By not considering this case of a rare, but very large crack, one may suggest that the probability of failure is not conservative. However, in the present case where inspections are regularly conducted it appears that the initial flaw size is not the only important factor. From Figure 15, it can be seen that the stringer has a residual strength at or above approximately 40 ksi even with cracks up to 1.5 in. present. According to Figure 8, the 40 ksi level is exceeded in the order of only 10^{-8} times per flight. Thus one large crack growing alone will contribute little to the probability of failure. Furthermore there is little chance that this single crack would evade detection. However, it was thought that by modelling a number of large cracks near the edge of the stringer, the number of large cracks at a future time would increase. This would increase the chances of one of them evading detection and growing to a size where there is an increased chance of failure. For this reason, the method of simulation used is thought to be conservative. The one remaining crack of the 93 expected that was not modelled should not make a significant contribution to the probability of failure as it is not amongst the 42 largest in the stringer.

An inspection was simulated for the initial cracks in each simulation, then the stringer 's residual strength was checked against a random load from the load exceedance distribution that was derived for RAAF usage. The remaining cracks after inspection were grown at 100 hour intervals. The interval used was increased in comparison to the simulations with no inspections because of the increased time taken for each simulation and the increased number of simulations that were needed to produce useful results. At

the end of each interval the residual strength was checked against the largest loads from 100 hours of flying. An inspection was simulated every 900 hours.

12. Probability of failure estimation from the Monte Carlo simulations

12.1 Assumed starting point of the simulations

The initial cracks present in the Monte Carlo simulations were based on the data from the LOT inspections. These occurred on aircraft A20-623 after 19265 flight cycles and on aircraft A20-627 after 18896 flight cycles. Table 1 indicates that the current number of flight cycles accumulated by all of the RAAF B707s is around 19,000. On the other hand, the number of flight hours varies much more, with aircraft A20-629 leading the fleet with 59435.7 hours. This is significantly greater than the flight hours when the LOT inspections took place on aircraft A20-627 and A20-623 (at 49411.5 and 54697.5 hours respectively). If this difference in flight hours between A20-629 and the LOT inspections were a true indication of the relative size of cracks present in the stringers of the aircraft, then one would expect the cracks A20-629 to be larger than those found at the time of the LOT inspections. However, a routine inspection of stringers 5 and 7 on A20-629 according to Service Bulletin A3395 at 58007 hours found no defects [17]. In fact the only defects found during recent HFEC inspections of fastener holes at the lower flanges of stringers 5 and 7 were cracks 0.25 in. and 0.08 in. long found in the stringers of A20-624 at 48967 flight hours [17, 18]. It seems that on the evidence of recent inspections the accumulated airframe hours of an aircraft are not necessarily a good indicator of the size of cracks present in stringers.

The assumed lognormal distribution of cracks sizes says that the largest crack present in a stringer will be at least 0.42 in. at least 25% of the time (see the cumulative distribution function in Figure 13). The cracks from this 25% of the simulations will contribute most to the calculated probability of failure, at least when there are no inspections. If these cracks were present during the routine HFEC inspections, there is a very good chance they would have been found because this crack size is greater than the 90/95 POD crack size. Thus it is fair to assume that the stringers in the RAAF fleet have damage that is less severe than the worst 25% of simulations. For this reason, it is assumed that it is safe to peg the probability of failure results to the last routine HFEC inspections (i.e. when the cracks in the aircraft's stringers were shown to be less severe than at least the worst 25% of simulations) or the LOT inspection for aircraft A20-623.

12.2 Assumed acceptable probability of failure

As was pointed out in Section 5, because the Monte Carlo simulations do not begin at the start of the aircraft's entire life, it was not possible to calculate the TPOF. However, the SFPOF was estimated from the rate at which the TPOF changed, and this quantity was compared to acceptable levels. JSSG-2006 states that the maximum acceptable level of structural failure per flight leading to loss of the aircraft is 10^{-7}[22]. The USAF also

indicates that limited exposure to a SFPOF between 10^{-7} and 10^{-5} is acceptable, but that it is unacceptable for the SFPOF to be above 10^{-5} at any time [23].

Based on an acceptable SFPOF of 10^{-7} for the entire aircraft, it was possible to estimate the acceptable SFPOF limit for the lower wing stringers by making a number of assumptions. It was assumed that there are ten locations on the B707 that contribute significantly to the probability of failure and that the lower wing stringers on each wing are equivalent to one of these locations. Thus the wing stringers on both wings were assumed to be limited to two tenths of the aircraft's acceptable risk level. This means that the acceptable risk level for the four adjacent stringers in a B707 were limited to a SFPOF of less than 2×10^{-8}.

12.3 Results of Monte Carlo simulations without inspections

The result of each of the simulations performed was a time to failure. For the cases where no inspections were assumed, 100,000 simulations were performed. The time to failure results from each set of simulations were converted into a TPOF using Equation 3. It should be noted that this gives the TPOF after the LOT inspections, not in the entire life of the aircraft.

The TPOF for a single stringer as a function of flight cycles is given for the cases where it was assumed there were no inspections in Figures 17, 18 and 19. Figure 17 gives the probability of failure for simulations related to the section of stringer adjacent to the assumed failure of a splicing stringer and Figure 18 gives the probability of failure for the remainder of the stringer. Figure 19 gives the probability of failure in the section of stringer inboard of WBL 59.24, where it is not possible to inspect the adjacent stringers. In the simulations associated with Figure 19, it was assumed that there was no failure of a splicing stringer adjacent to this uninspectable area. In each of Figures 17-19, the TPOF is plotted on a log scale. It can be seen that most of the results before 3000-3500 flight cycles increase at a near linear rate on a log scale.

The TPOF results were used to make an estimate of the SFPOF. If the TPOF as a function of time is represented by *G(t)*, then the rate at which the TPOF changes per flight is the derivate of *G(t)*:

$$SFPOF = g(t) = \frac{dG(t)}{dt} \qquad \textit{Equation 9}$$

The SFPOF was estimated with an approximation of *g(t)*:

$$SFPOF = g(t) \approx \frac{\Delta TPOF}{\Delta t} \qquad \textit{Equation 10}$$

The average TPOF was calculated over 127 flight cycle intervals for each case given in Figures 17-19. This averaging was done to reduce any localised effects of the Monte Carlo method. These average TPOF values were used to calculate *ΔTPOF* in Equation 10. The SFPOF was then estimated at successive times by dividing each *ΔTPOF* by the interval of 127 flight cycles. The SFPOF values calculated by this method are included as the red markers in Figures 17-19. These cases are for a single stringer and no inspections.

In Figures 17-19 there are no results available for TPOF below 10^{-5}. This was a result of the number of simulations performed (100,000). Because of the limits on the TPOF, there were also limits on the SFPOF results available. Figure 17 indicates that a SFPOF was calculated for times after approximately 1500 flight cycles for the section of stringer adjacent to the failure of a splicing stringer. The SFPOF was only available after approximately 1000 flight cycles for the remainder of the stringer (see Figure 18) and the SFPOF was only available after approximately 2500 flight cycles for the section of stringer inboard of WBL 59.24 (see Figure 19). However, the SFPOF results in all three cases appear to increase at a steady rate on the log-scale that they are plotted on, up to a SFPOF of approximately 10^{-4}. It was therefore assumed that the SFPOF could be predicted for times prior to those available from the Monte Carlo simulations with the exponential rate that occurred for SFPOF less than approximately 10^{-4}. For this purpose of extrapolating the available SFPOF results, exponential functions were fitted by linear regression analysis of the log SPOF and flight cycles. The relationships were derived using SFPOF data below approximately 10^{-4}. The following relationships between the SFPOF and flight cycles (t) were derived:

1. Region adjacent to the failure of a splicing stringer :

$$SFPOF(t)_{Near\ failure} = 2.91\times10^{-13}e^{0.0067t} \qquad \textit{Equation 11}$$

2. Remainder of the stringer:

$$SFPOF(t)_{Remainder} = 2.92\times10^{-9}e^{2.68\times10^{-10}t^3-6.45\times10^{-7}t^2+2.48\times10^{-3}t} \qquad \textit{Equation 12}$$

3. Region of the stringer inboard of WBL 59.24:

$$SFPOF(t)_{WBL\ 59.24} = 9.71\times10^{-16}e^{0.007062t} \qquad \textit{Equation 13}$$

These relationships are plotted in blue in Figures 17-19 and Equations 11 to 13 were used in subsequent calculations of the SFPOF of an aircraft's four adjacent stringers.

The alternative to the extrapolation used would be to increase the number of simulations for each case considered. However, an order of magnitude increase in simulations would be required to reduce the lower bound of the available results by an order of magnitude. This means that the computation time would be ten times longer, so it was thought that this extra computation time was not practical, especially when the rate at which the SFPOF was increasing appeared to be quantifiable.

An estimate can also be made of the SFPOF for an entire stringer by taking into account the chances failure of both of the section of stringer adjacent to a failure of a splicing stringer and the remainder of the stringer. In this estimate it was assumed that the probabilities that failure would occur in either of these regions were independent. In truth the probability of failure of the two regions are not independent, because both regions are in the same load path. This means that one region will always break before the other and there is no possibility of both regions failing on the same stringer. However, the assumption that the two failure probabilities are independent is conservative. For independent events the chances of failure occurring in either region is one minus the

probability of failure occurring in neither region. For small probabilities of failure this can be estimated as the sum of the two failure probabilities:

$$SFPOF(t)_{stringer-no\ inspections} = 1-(1-SFPOF_{Near\ failure})(1-SFPOF_{Remainder})$$
$$\approx SFPOF_{Near\ failure} + SFPOF_{Remainder} \qquad \textit{Equation 14}$$
$$\approx 2.91\times10^{-13}e^{0.0067t} + 2.92\times10^{-9}e^{2.68\times10^{-10}t^3-6.45\times10^{-7}t^2+2.48\times10^{-3}t}$$

By multiplying Equation 14 by four, the contribution to the aircraft's overall SFPOF from the four sets of splicing and adjacent stringers, assuming no inspections, was calculated. This SFPOF estimate is shown in Figure 20 along with the TPOF and piecewise estimate of the SFPOF that were derived by adding the probability of failure contributions from the different regions of the stringer in a manner similar to that given in Equation 14. From Figure 20 it can be seen that the SFPOF reaches the maximum acceptable level of 2×10^{-8} after only 200 flight cycles when it is assumed there are no inspections performed.

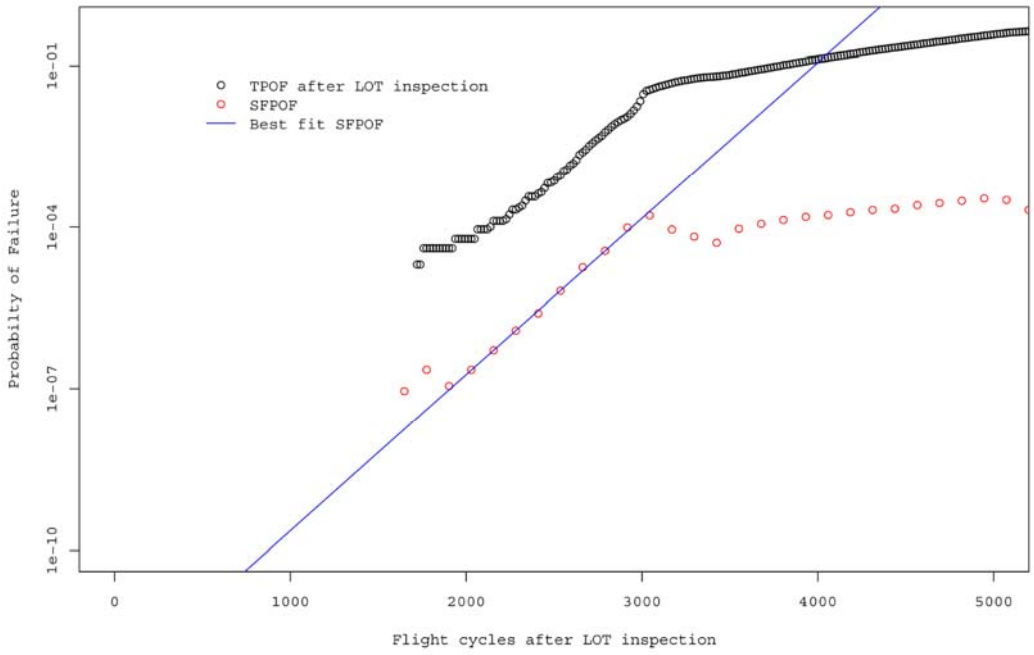

Figure 17 - Probability of failure versus flight cycles for the section of stringer adjacent to the assumed failure of a splicing stringer (assuming no inspections).

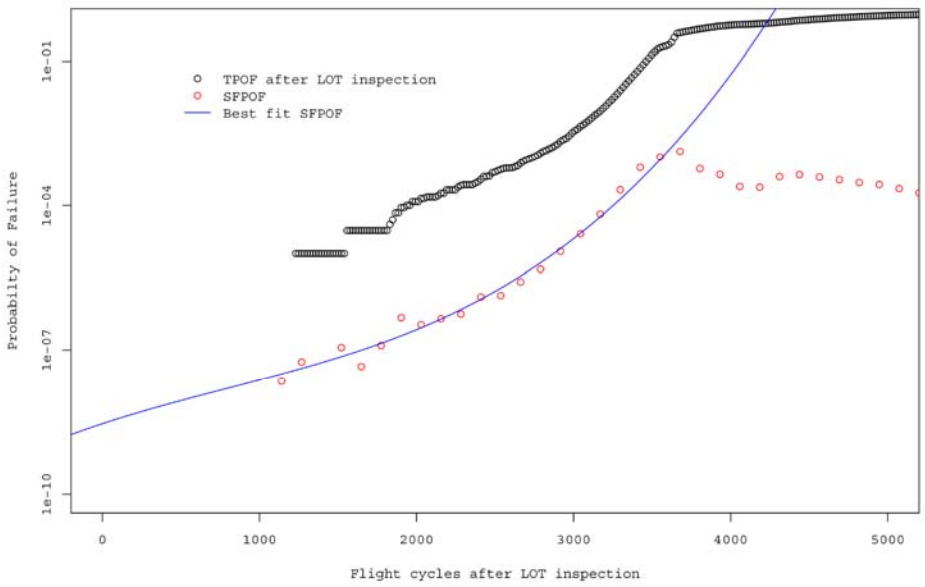

Figure 18 - Probability of failure versus flight cycles for the section of stringer not adjacent to the assumed failure of a splicing stringer (assuming no inspections).

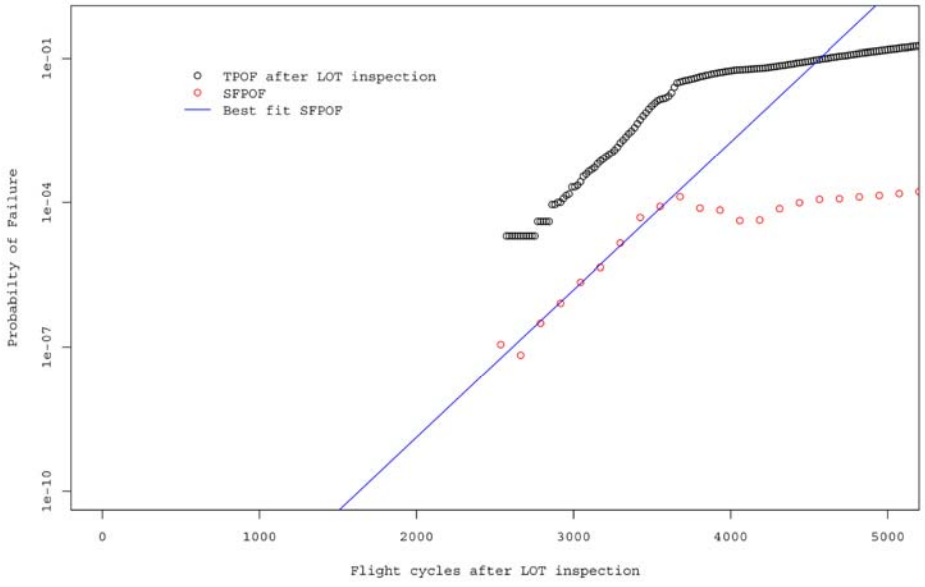

Figure 19 - Probability of failure versus flight cycles for section of stringer inboard of WBL 59.24 (which is not inspectable).

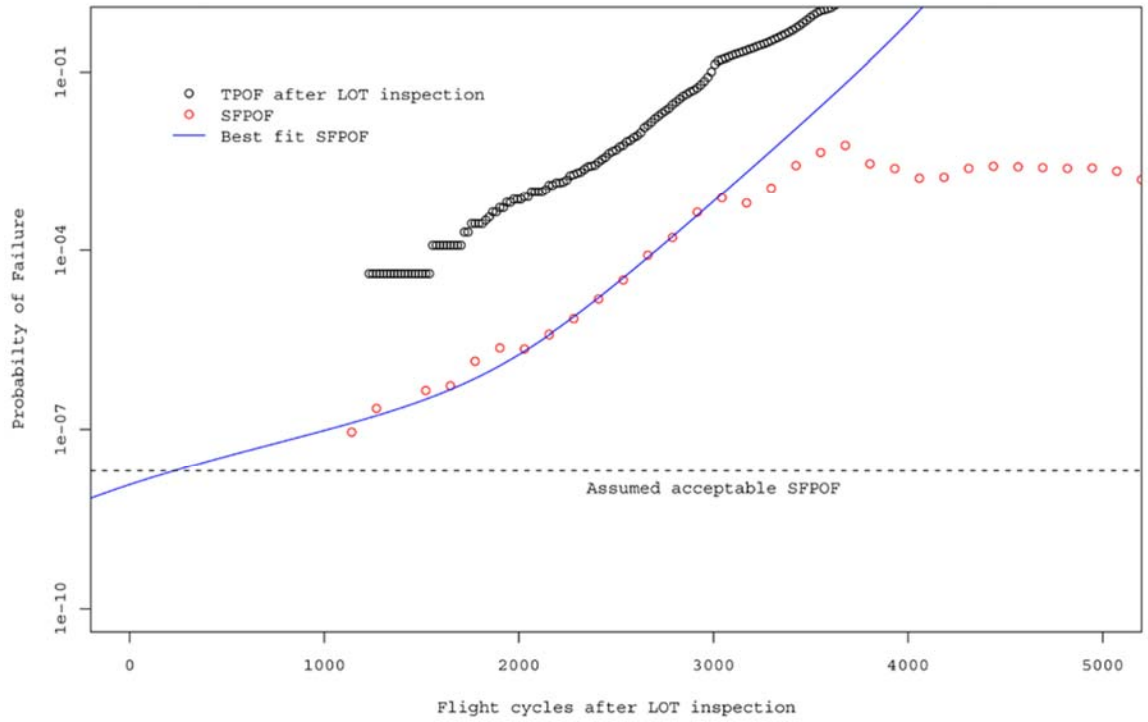

Figure 20 - Probability of failure versus flight cycles for the four adjacent stringers in each B707 (assuming no inspections).

12.4 Results of Monte Carlo simulations with inspections

Monte Carlo simulations were also performed with HFEC inspections simulated at 900 hour intervals for the region of stringer adjacent to the failure of a splicing stringer and for the remainder of the stringer. In each case 200,000 simulations were performed. A greater number of simulations were performed in comparison to the simulations where no inspections were assumed because it was found that there were far fewer failures in the time interval investigated (approximately 5000 flight cycles). Thus 100,000 extra simulations were performed in order to get more data to describe the rate at which the probability of failure increased. Even with the additional simulations, only three failures were observed in both regions of the stringer combined before 5000 flight cycles had elapsed. Because of the small number of failure observations, the TPOF results were generated for both regions using Equation 3 and these results were combined by addition. The TPOF for the entire inspected stringer is given in Figure 21. The TPOF increased by only 3/200,000 in the 5000 flight cycle period that was considered.

Because of the small amount of data available for the inspected case, it was not possible to estimate the SFPOF with the piecewise calculation of the local slope of the TPOF curve that was done for the uninspected cases. Observing that the log of the TPOF from uninspected cases increased almost linearly, it was assumed that the log of the TPOF for the inspected

case also increased at a linear rate. With this assumption a linear regression was performed (using the log TPOF) to derive an exponential relationship between the TPOF and flight cycles:

$$TPOF(t)_{Inspected} = 8.60 \times 10^{-7} e^{0.00065t} \qquad \textit{Equation 15}$$

The SFPOF can then be derived from Equation 15 since it is the derivative of the TPOF function as was shown in Equation 9. The derivative of the assumed exponential function that represents the TPOF is given by:

$$g(t) = \frac{d}{dt} c\, e^{ax} = ca\, e^{ax} \qquad \textit{Equation 16}$$

Thus from the coefficients given in Equation 15, the SFPOF as a function of flight cycles is:

$$SFPOF(t)_{Inspected} = 5.59 \times 10^{-10} e^{0.00065t} \qquad \textit{Equation 17}$$

The variation of the SFPOF with flight cycles for the case of an entire stringer that is inspected every 900 hours is given in Figure 21. The SFPOF given by Equation 17 was multiplied by four to give the contribution of the four adjacent stringers in the B707's two wings to the aircraft's SFPOF. This is plotted in Figure 22. This Figure indicates that the SFPOF will reach the unacceptable threshold after approximately 3500 flight cycles.

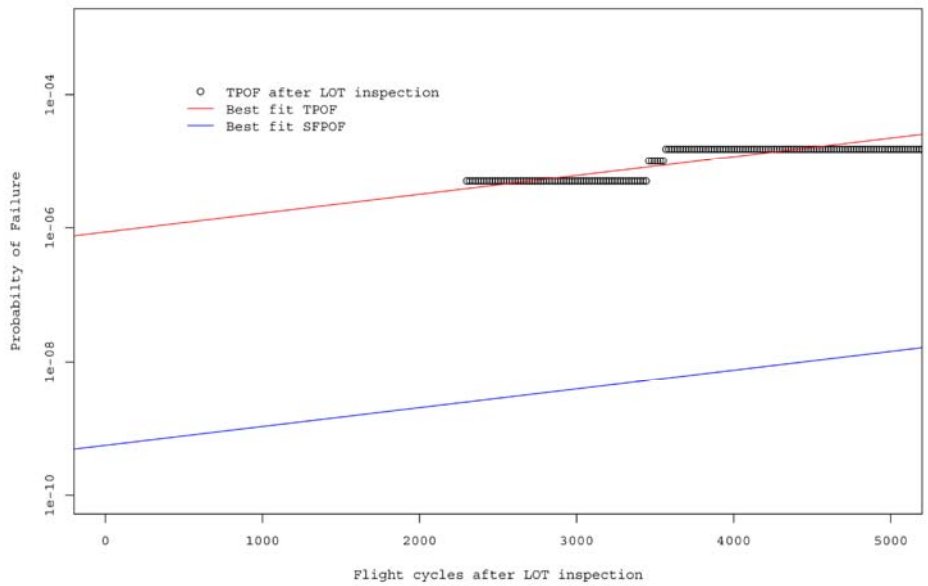

Figure 21 - Probability of failure versus flight cycles for an entire adjacent stringer assuming HFEC inspections at 900 hour intervals.

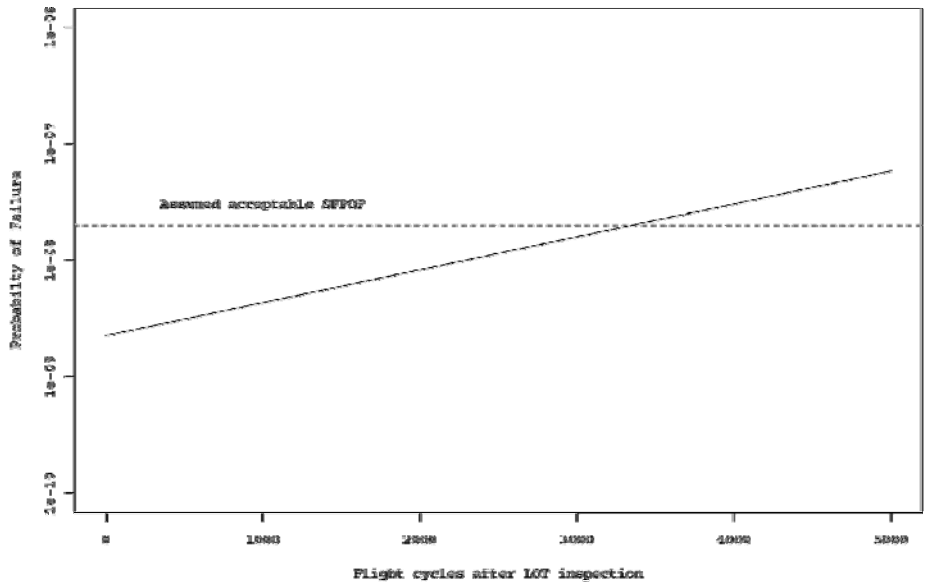

Figure 22 - SFPOF versus flight cycles for the four adjacent stringers in each B707 assuming the whole adjacent stringer is inspected with HFEC every 900 hours.

12.5 Estimate of the SFPOF under recommended RAAF inspections

In this section the contribution of the adjacent stringers to a RAAF B707's SFPOF is estimated from a combination of the probability of failure results that were derived above. The results are derived assuming that the adjacent stringers are inspected every 900 hours with HFEC around each fastener hole, except for the region inboard of WBL 59.24 where no inspections are possible. The results from the previous section are combined by addition with the assumption that the failure probabilities of different regions of the stringer are independent and that the probabilities of failure that are of interest are small.

Since the Boeing routine inspections of the adjacent stringers (as per Service Bulletin A3395) cover only fasteners inboard of WS 733, it was assumed that all critical fasteners were inboard of this location. The stringers were also assumed to start at the inboard edge of the wing (BBL 76.45). Thus the length of stringer containing critical fasteners is approximately:

733-76.45 = 656.55 in.

There may be a slight error in this estimate due to the assumption that WS 76.45 corresponds to BBL 76.45. The proportion, *l*, of the stringer that is not inspectable (inboard of WBL 59.24) is approximately:

$$l = \frac{59.24}{656.55} = 0.09 \qquad \textit{Equation 18}$$

The overall probability of failure is the combination of the inspectable and uninspectable regions of the stringer. The probability of failure for the uninspectable region is the combination of:

1. The probability of having the failure of a neighbouring splicing stringer in this uninspectable region multiplied by the probability of failure for an uninspected length of stringer near to a failure of a splicing stringer. A single failure was assumed in each splicing stringer so the probability that it this failure would occur in the uninspected region is *l*. Equation 11 gives the probability of failure for the region near the failure of a splicing stringer.
2. The probability of not having a splicing stringer failure adjacent to the uninspectable region (*1- l)*, multiplied by the probability of failure for uninspected cracks in a 59.24 in. span, which is given by Equation 13.

In truth, if there were a failed splicing stringer in the uninspectable region, there would be 34 in. of the adjacent stringer at an increased stress level and 25 in. at the normal stress level. In the formulation above, the 25 in. at the normal stress has been neglected. Comparison of Figures 17 and 19 shows that the probability of failure for a 34 in. span of stringer near the failure of a splicing stringer is an order of magnitude greater than the probability of failure for a 59.24 in. span that is not near a splicing stringer failure. The difference would be even more pronounced for a 25 in. span. Thus to neglect this region will not make a great difference to the overall estimate.

The probability of failure for the remainder of the stringer, which is inspected, was estimated with Equation 17. This equation calculates the SFPOF for the whole stringer rather than the proportion of stringer that is inspected (1- *l*) so it is a little conservative. There may also be part of the stringer outside of WS733 that is not inspected. However it is assumed that cracking in this region is not significant since Service Bulletin 3395 does not prescribe inspection in this area and a failure in this region of the stringer would not cause a failure that would lead to the loss of the aircraft.

Combining the failure probabilities outlined above and multiplying by four to account for each B707's four adjacent stringers gives the following estimate of the contribution of the adjacent stringers to the aircraft's SFPOF:

$$SFPOF(t)_{RAAF\_B707} = 4(5.59\times10^{-10}e^{0.00065t} + l\ 2.91\times10^{-13}e^{0.0067t} + (1-l)\ 9.71\times10^{-16}e^{0.007062t}) \qquad \textit{Equation 19}$$

The estimate given by Equation 19 is plotted in Figure 23. According to this plot, the SFPOF reaches the unacceptable threshold after 1750 flight cycles. If it is assumed that the simulations can be pegged to their last routine inspection or the LOT inspection for A20-623 (for the reasons given in Section 12.1), then this will mean that each B707 will be able to fly another 1750 flight cycles after their last routine inspection with their lower wing stringers at an acceptable risk level. Of course, this result is based on ongoing routine inspections at 900 hour intervals.

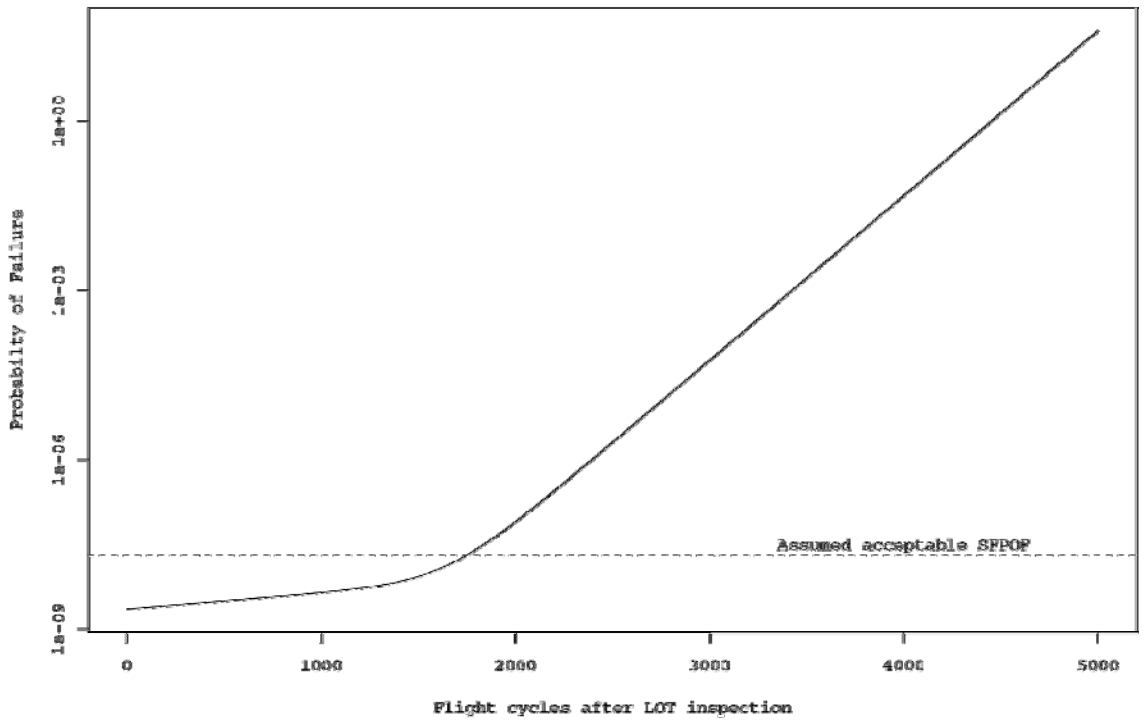

Figure 23 - SFPOF versus flight cycles for the RAAF B707 lower wing stringers when the adjacent stringers are inspected with HFEC outboard of WBL 59.24 every 900 hours.

13. Summary of assumptions made in the analysis

This section lists the assumptions made during the risk analysis of the B707 lower wing stringers.

1. Using the typical geometry for the lower wing stringers given in Figures 2 and 3 will represent the entire stringer well enough to yield accurate or conservative probability of failure estimates.
2. A failure of the lower wing stringers 4 and 5 or 7 and 8 on a single wing is required to cause failure of that wing. Failure of the wing will cause failure of the aircraft. Previous analysis by the USAF [1] indicates that failure of the wing skin equivalent to two stringer bays is also required in addition to these stringer failures to cause failure of the wing so this assumption may be conservative.
3. There is a single complete break in stringers 4 and 8 in each wing. This assumption is likely to be conservative, at least in the case of an entire Monte Carlo simulation, because regular inspections according to Service Bulletin 3226 should be able to detect a broken stringer. Thus it is unlikely that cracks in an adjacent stringer near the failure of a splicing stringer would grow for a long period of time under the influence of this failure. In the Monte Carlo simulations performed, it was assumed that the loads on this portion of the adjacent stringer (next to the assumed failure of the splicing stringer) were always increased by this failure. Also, routine

inspections of the splicing stringers over approximately the last eight years have not detected a complete failure of a splicing stringer [17]. Thus it is unlikely that any of the splicing stringers were failed at the start of the simulations as was assumed in the analysis. The one area where this assumption may be realistic and not conservative is in the region of stringers inboard of WBL 59.24 where LFEC inspection of stringers 4 and 8 is not possible [3]. In this region there is no way to check if stringers 4 and 8 have failed, so it may be safe to assume that a splicing stringer has possibly failed in this region.

4. The lower wing skin is intact. It is assumed that if a failure of the skin occurs, the crack will be large enough to be found during flight line inspections. Fuel leaks from these large skin cracks should also increase the likelihood that the cracks are found. The chance that a skin failure will be followed by a stringer failure, then complete failure of the wing in a single flight (i.e. before the skin failure can be found in routine flight line inspections) is considered remote. This assessment is based on the distribution of expected crack sizes. Most cracks are expected to be small and there is a low probability that one crack, let alone two cracks will become critical in a single flight. Skin cracks may also be detected before they reach a critical size, because there will probably be fuel leaks. A final reason to believe that the skin will be intact is the evidence of the LOT inspections which found that in comparison to the stringer cracks, skin cracks were far less numerous and those cracks that were found were small.
5. The risk analysis is based on cracking from fasteners between the lower flanges of the lower wing stringers 4,5, 7 and 8, and the lower wing skin only.
6. The assumed failures of the splicing stringers are at different span-wise locations and will not influence each other.
7. The stress in an adjacent stringer 17 in. either side of the assumed failure of a splicing stringer is 1.06 times the stress normally present. In fact, finite element analysis indicates that this is the peak increase of the stress level and most of the region will be at a lower stress.
8. The load exceedances experienced by the E-8A in a single flight adequately describe the load exceedances for a single flight of a RAAF B707. This assumption is likely to be conservative as the E-8A has a much longer flight duration (9.2 hours versus 2.76 hours) so it is likely to experience more loads per flight. If the environment and mission type of a E-8A was similar to that of a RAAF B707 then it would be much more likely to see a large load in a flight because it experiences more loads per flight.
9. A crack was assumed to be present on both sides (fore and aft) of the critical fastener hole. This is likely to be conservative as the LOT inspections indicated that most of the holes where cracks were found had a crack on only one side of them (see Figure 16).
10. It was assumed that the larger of the two cracks present at a fastener hole was on the side of the hole that is closest to the edge of the stringer. This assumption was made because a crack on this side of the hole is likely to grow faster and give the stringer a lower residual strength. This is due to it having a larger geometry factor than a crack that is growing toward the central stiffener.
11. When the initial crack nearest to the outer edge of the stringer was predicted by the lognormal crack size distribution to be larger than the edge distance between the

fastener hole and the outer edge of the stringer, the crack size was reset to be equal to the edge distance.

12. The total crack size at a hole is the sum of the two cracks assumed to be present. When the sum length of these two cracks was less than the edge distance between the hole and the edge of the stringer, it was assumed that these cracks on either side of the hole are equivalent to a single crack on the side of the hole that is closest to the edge of the stringer. This assumption was made so that the J-STARS crack growth and residual strength functions could be used in the analysis. This assumption is conservative.
13. For the assumed case of no inspections in the region near to a failure of a splicing stringer, it was assumed that the largest two of the estimated four cracks in this region were situated on either side of one hole. This is likely to be conservative as the LOT inspections indicated that most times there was only a single crack at a hole. Also, the chance of the second largest crack being located at the same hole as the largest crack is very unlikely.
14. For the assumed case of no inspections in the regions of the adjacent stringer that are not affected by the failure of a splicing stringer, it was assumed that the largest crack is paired with any other of the 93 expected cracks.
15. In the region of the stringer inboard of WBL 59.24 where no inspections are possible, it was assumed that the largest crack is paired with any other of the 6 expected cracks.
16. It was assumed in the Monte Carlo simulations that cracks smaller than 0.4 in. long cannot be found using the HFEC inspection around each fastener head (used on stringers 5 and 7). It was also assumed that cracks that are 0.4 in. long or longer can be detected 90% of the time using this HFEC technique.
17. It was assumed in the Monte Carlo simulations that cracks found during inspection are repaired and this repair removes the crack completely. This assumption is unlikely to make much difference to the overall probability of failure calculation, because the flaws introduced after repair are unlikely to grow to be as big as the cracks already present after approximately 19,000 flight cycles.
18. For the assumed case of HFEC inspections every 900 hours in the region of the stringer that is adjacent to the failure of a splicing stringer, it was assumed that the largest two cracks were at separate holes and the other two cracks present in this region were on the other side of these holes.
19. For the assumed case of HFEC inspections every 900 hours in the region of the stringer that is away from the failure of a splicing stringer it was assumed that the largest forty-six cracks were at separate holes and forty-six other cracks present in this region were on the other side of these holes. The omission of one of the expected 93 cracks in this region of stringer from the analysis is assumed to have little effect on the probability of failure calculated, because it is one of the 43 smallest predicted cracks.
20. The probability of failure estimates can be pegged to the time of the LOT inspections for A20-623 and the time of the last HFEC inspection of stringers 5 and 7 according to Service Bulletin A3395 for the other active RAAF B707s.
21. The SFPOF results that were derived from the Monte Carlo simulations may be extrapolated below the lower limit of these data. It is assumed that this extrapolation gives an accurate estimate of the SFPOF.

22. The failure probabilities of different regions of the adjacent stringers are independent. This is not true but it is conservative.

14. Discussion of results

Comparison of the results in Figures 17-19, which give the probability of failure when no inspections are assumed, shows the influence of the number of cracks in the region considered. The probability of failure when the whole stringer was considered (excluding the region adjacent to a splicing stringer failure - see Figure 17) was much greater than when only 59.24 in. of the stringer was considered (see Figure 19). This is because there is a much greater likelihood of there being a large crack in a large region, which has many more cracks present. This was also the reason why the probability of failure was initially lower in the region adjacent to the failure of a splicing stringer (see Figure 18) than the remainder of the stringer (see Figure 17). At later stages after the LOT inspections, the probability of failure from the region adjacent to the failure of a splicing stringer was greater than the remainder of the stringer. This was probably caused by the increased stress in this region growing the largest crack present at an increased rate (in comparison to the remainder of the stringer). Because of the more rapid crack growth, the largest crack in this region becomes the largest in the stringer after a certain number of flight cycles. The region of stringer neighbouring the failure of a splicing stringer may also have become critical after a period of time because of the assumption that the two largest initial cracks were at the same critical fastener hole in this region. This may have been a more conservative assumption than the initial case for the remainder of the stringer where it was assumed that the largest crack was paired with any other present.

The probability of failure of an entire stringer when it is inspected with HFEC around each fastener at 900 hour intervals is very low. Even if the assumed linear increase in the TPOF is incorrect, the TPOF results (see Figure 21) certainly show that the rate of increase is low over the 5000 flight cycle life considered. Thus this approximation is unlikely to greatly affect the accuracy of the results.

The probability of failure with inspections is low because of a number of factors. Examination of the residual strength (see Figure 15) along with the stress exceedance probability (see Figure 8) functions indicate that there is a SFPOF of greater than 10^{-8} when the crack is greater than the 90/95 POD. In any one flight there is a limited probability that there will be a crack in the stringer that is greater than the 90/95 POD. Early in the life of the stringer (after the LOT inspections), the initial lognormal crack size distribution indicates that it is rare for a crack to be that large. As the cracks grow, the regular inspections ensure that cracks larger than the 90/95 POD are removed from the stringers. Inspections at a frequency of 900 hours ensure that cracks for which the SFPOF is greater than 10^{-8} do not exist for a long period of time.

When the uninspected and inspected results were combined to approximate the case where inspections can only be carried out outboard of WBL 59.24, it was found that the uninspected region dictated the life until the unacceptable SFPOF threshold was reached. It can be estimated from a comparison of Figure 22 with Figure 23 that the aircraft could

safely fly approximately an extra 1750 flights if the whole stringer was inspected. Although the assumption that each splicing stringer has failed is conservative for most of the stringer, because LFEC inspections will verify that there are no failures at each DM, it may not be so conservative in the uninspectable region inboard of WBL 59.24. In this region there is no way to confirm that there has not been a failure of a splicing stringer. Since this region determines the remaining life of the stringers (according to the SFPOF threshold), the assumption of a possible broken stringer appears safe.

15. Recommendations

It is recommended that HFEC inspections similar to those specified in Service Bulletin 3395 be carried out on stringers 5 and 7 of each aircraft at every scheduled DM. In addition, it is also recommended that remedial maintenance action is taken on the lower wing stringers of RAAF B707 fleet aircraft or that aircraft are retired from service before they reach 1750 flights cycles after their last DM (except in the case of A20-623 which should be pegged against the LOT inspections). It would be acceptable for these actions to be delayed by a short period of time (< 100 flight cycles) according to the USAF recommendation that it is acceptable to fly at a SFPOF between 10^{-7} and 10^{-5} for a short time. In this recommended 100 hour period the TPOF of the lower wing stringers will only increase by approximately 3.5×10^{-6}.

Since the uninspectable region inboard of WBL 59.24 dictates the remaining life of the aircraft, inspection of this area, though difficult, may increase the remaining life of each aircraft. Thus if the above maintenance or retirement options are not acceptable, a once off inspection of this region to ensure with a high degree of confidence that no cracks larger than the 90/95 POD crack size are present in this area could ensure safety for a further time period. By ensuring that there is little possibility that there are any cracks that have a significant probability of failure present, the probability of failure calculated in this document may be adjusted to allow an additional period of flying.

Another possible way to extend the remaining life of aircraft beyond 1750 flight cycles is to conduct another sampling inspection using BHEC inspection of selected holes, as was done for the LOT inspections, at a later time. Because the assumed initial flaw cracks sizes and crack growth in this analysis are conservative, it is likely that the cracks present in the stringers at some future time will be smaller than predicted. Thus by re-determining the crack size distribution for each aircraft and repeating the analysis in this report (keeping all other inputs the same), additional life from the time of the new inspections will be gained. This inspection should be conducted well in advance of the time when each aircraft's allotted 1750 flight cycles are due to elapse.

Since it is assumed that a failure of both stringers 4 and 5 or 7 and 8 plus two stringer bays of wing skin are required to cause failure of the wing, inspections of stringers 4 and 8 plus the wing skin will also reduce the risk of failure. The RAAF currently conducts LFEC inspection of stringers 4 and 8 according to Service Bulletin 3226. It is recommended that these LFEC inspections continue to be conducted at each DM. The current RAAF LFEC inspection involves only a scan along the line where the wing skins join at stringers 4 and

8. The 90/95 POD crack size in this case is equivalent to the failure of one of the stringer's flanges. To improve the POD of inspections and thus reduce the chances of failures in stringers 4 and 8, it is recommended that the RAAF also adopt a technique of "spotting" next to fasteners as described in Section 3. A LFEC inspection of the lower wing skins in the vicinity of fasteners attaching stringers 4, 5, 7 and 8 will also mitigate against the risk of failure.

16. Conclusion

A structural risk assessment of the lower wing stringers of RAAF B707 aircraft was performed to evaluate their safety when stringers 4 and 8 are maintained with Low Frequency Eddy Current inspection, stringers 5 and 7 are maintained with High Frequency Eddy Current inspection around each of their fastener holes and inspections of all critical stringers are only possible outboard of WBL 59.24. The risk assessment was focussed on fastener holes between the lower flanges of stringers 4, 5, 7 and 8 and the lower wing skin. These stringers were found to be critical in previous risk assessments of the B707 lower wing. From the previous risk analyses it was determined that the failure of stingers 4 and 5 or 7 and 8 was required along with cracking of two stringer bays of wing skin to cause failure of the wing. Considering the low chance of finding cracks in stringers 4 and 8 with LFEC, plus the lack of crack growth data available for these stringers, it was decided to simplify the analysis by assuming that each of these stringers had a single break in them.

As a result of this simplification, the risk assessment reduced to a problem of determining the probability of stringer 5 or 7 failing. For this purpose, Monte Carlo simulations of crack growth in these stringers were performed. The initial condition of stringers 5 and 7 was determined from the Life Of Type sampling inspection of fastener holes in these stringers that occurred over the years 1999/2000. The cracks found in these inspections were used to determine a lognormal probability distribution that described the expected sizes of cracks in stringers 5 and 7 at the start of the analysis. Cracks were sampled from this distribution to describe the initial condition of the stringer in each simulation.

Each simulation was performed by growing the cracks present in a stringer until it failed. The failure of the stringer was determined by the size of the cracks present and the maximum load it had experienced in the preceding flights. The deterministic function that was used to grow cracks was based on a crack growth curve for stringers 5 and 7 used in a previous United States Air Force risk analysis. This crack growth was adjusted for the differences in RAAF and USAF aircraft usage. The maximum load simulated for each flight was determined from a probability of load exceedance function. This function was determined from the load exceedances per flight of USAF aircraft.

Because it was assumed that there was a failure of stringer 4 and 8 in each wing, it was necessary to determine the effects of this on stringers 5 and 7. A finite element analysis determined that the stress in stringer 5 directly neighbouring a break in stringer 4 increased by a factor of 1.06. However, it was found that the level of increased stress diminished rapidly and only approximately 34 in. of stringer 5 was affected by the break.

As a result of this analysis, two sets of Monte Carlo simulations were used to calculate the stringer's probability of failure, one set for the 34 in. region of stringer next to the assumed failure of stringer 4 or 8, plus another set for the remainder of the stringer. The crack growth and load exceedance functions were adjusted for the increase in stress in the region near a failure of stringer 4 or 8 in the first set of simulations.

To take account of the limited coverage of RAAF inspections, simulations were also performed assuming both High Frequency Eddy Current inspections around each fastener at 900 hour intervals and assuming no inspections. The completed simulation results were combined to estimate the risk of failure for the assumed RAAF case of a single break in stringers 4 and 8 with stringers 5 and 7 only inspectable outboard of WBL 59.24. The results of the Monte Carlo simulations were used to determine the Total Probability of Failure from the beginning of the simulations. These results were then used to estimate the Single Flight Probability of Failure. It was found from this estimate that the lower wing stringers of RAAF B707s are safe for 1750 flight cycles from the time of their last inspection (previous to this report, except for aircraft A20-623, which should be pegged to the time of the Life Of Type inspections).

17. References

1. Anon., "Structural Evaluation Of The E-8C J-STARS Wing Lower Surface", Technical Interchange Meeting Presentation, Boeing Product Support Division, Wichita, 4 Apr. 1996.
2. Tong, C., Amaratunga, R., Graham, D. and White, P., "Probabilistic Assessment of the Failure of Fastener Holes in Wing Stringers of RAAF B707 Aircraft", DSTO-TR-1161, July 2001.
3. Young, G. D., "Review of LFEC External Inspection Intervals For Lower Wing Stringers, RAAF B707 Aircraft", ASI A20/99001 Pt 1 (31), Minute, Directorate General Technical Airworthiness – Australian Defence Force, 15 Aug 2003.
4. Boeing 707 Service Bulletin A3395, Wing – Lower Skin and Stringer Inspections at Stringers 5 and 7, Rev. 4, 28 Oct. 1999.
5. Boeing 707 Service Bulletin 3226 - Wing Lower Skin Splice Stringer, Rev. 5, 25 Nov. 1981.
6. "707-320 Structural Teardown Inspection", S5685, Model 707/720 Structures Meeting – Boeing Presentations, Boeing Commercial Airplane Company, 23 Oct. 1975.
7. Boeing 707 Supplemental Structural Inspection Document, D6-44890, Rev. P, AAP 7211.019-2-17, Apr. 1994.
8. Jackson, P., "POD Curves for B707 Inspections", letter to David Graham, DSTO File: B2/166, 9 Jun. 1999.
9. POD Assessment of NDI Procedures Using a Round Robin Test, AGARD Report 809, Jan. 1995.
10. Usui, K. K., "Engineering Summaries in Support of the Supplemental Structural Inspection Document for High Time Aircraft – Model 707/720", D6-48444, Boeing Commercial Airplane Company, Seattle, 1 Aug. 1981.

11. Romero, V and Ellis, C., "RAAF 707 Life of Type Study Fleet Sampling Inspection Program", Iss. A, C5359, QANTAS Airways Limited, 13 Apr. 2001.
12. Luzar, J. and Hug, A., "Lower Wing Disassembly and Inspection Results of Two High Time USAF B707 Aircraft", Proceedings of the USAF Aircraft Structural Integrity Program conference, 1996.
13. Anon., "Risk Assessment of B-707 Joint Stars Aircraft", USAF presentation.
14. Montgomery, D. C. and Runger, G. C., "Applied Statistics and Probability for Engineers", John Wiley and Sons, USA, 2003.
15. Stephenson, A., "A User's Guide to the evd Package (Version 1.2)", Lancaster University, 2002.
16. Gumbel, E. J., "Statistical Theory of Extreme Values and Some Practical Applications", Technical Report Series 33, National Bureau of Standards, Feb. 1954.
17. Charlesworth, S. ,"Lower Stringer Inspection Summary", DSTO file 2005/1022890.
18. Ellis, C., "QANTAS Engineering Authority – Crack in RH lower stringer 5 fastener hole at WS 348", EA SS3699, QANTAS, 22 Feb. 2000.
19. Murtagh, B. J., "RAAF B707 Fatigue Assessment for Usage to December 2002", AeroStructures, 14 Apr. 2003.
20. Anon. , "AAR Damage Tolerance Evaluation, Technical Report 880369", Israeli Aircraft Industries, December 1989.
21. Anon., "Metallic Materials and Elements for Aerospace Vehicle Structures", MIL-HDBK-5j, United States Department of Defence, 31 Jan. 2003.
22. Anon., "Joint Service Specification Guide, Aircraft Structures", JSSG-2006, 30 Oct. 1998.
23. Babish, C., Alford, R. and Thomsen M., "Probabilistic Approach to Support the Force Management Decision Making Process", 2003 Aircraft Structural Integrity Program Conference Proceedings, 3 Dec. 2003.
24. Bailey, T., "Introduction to Lap Joint and Doubler Bolt Load Transfer Analysis Program BOLTRAN ", IFO 0030, Bombardier Inc., May 1992.

Appendix A: Description of the finite element model used to estimate the effect of a splicing stringer failure

A.1. Model geometry

The finite element model used to estimate the effect of a failed splicing stringer is shown in Figure A1. A panel of wing skin attached to a number of stringers has been modelled. Each stringer modelled has been numbered and the edges of the panel have been labelled A-D to aid description of the model. The geometry is based on that given in Figure 2. The spacing between the vertical stiffener of each stringer is 7 in. There was also another 3.5 in. of skin outside of the vertical stiffener of stringers 2 and 10. Thus the total width of the panel modelled was 70 in. (this would be in the chord-wise direction on the aircraft). The model is also 100 in. long in the span-wise direction (z in Figure A1).

The skin and stringers were modelled as shell elements. The skin thicknesses used in the model are shown in Table A1.

Fasteners connecting the skin and stringers were modelled as spring elements. Separate elements were used to model the shear stiffness in the x-direction, the shear stiffness in the z-direction and axial stiffness in the y-direction. The skin and the base of the stringers were separated by 0.01 in. Spring elements joined nodes at the locations of fasteners. The spacing of fasteners in stringers 4, 5, 7 and 8 was according to the rivet pitch shown in Figure 3. The single row of rivets in stringers 2, 3, 6, 9 and 10 were spaced 1.2 in. apart in keeping with the pitch given in the J-STARS risk analysis [1].

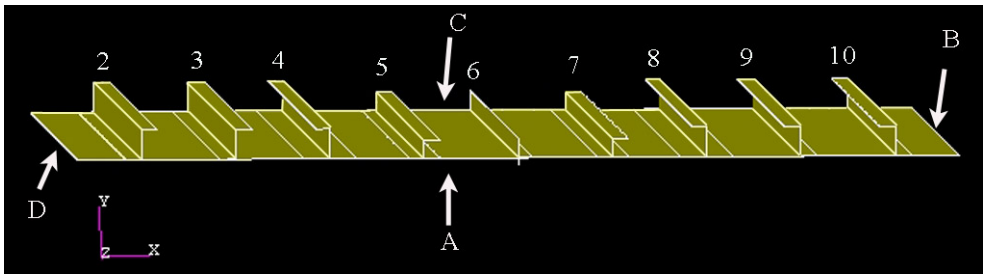

Figure A1 – The finite element model used to predict the effect of a failed splicing stringer.

Table A1 - Skin thicknesses used in the finite element model.

Skin section	Thickness (in.)
Between stringers 5 and 7	0.18
Under stringers 5 and 7	0.375
Forward and aft of stringers 5 and 7	0.16

A.2. Material properties

The skin and stringers were all given a Young's Modulus of 10.3×10^3 ksi and a Poisson's Ratio of 0.33. These are the figures given for 7075 aluminium alloy in Reference 1. Because there is little difference between the stiffness of different aluminium alloys, it was assumed that this was applicable to the skins as well.

The shear and axial stiffness of the fasteners were also modelled. The shear flexibility, C, of the fasteners was calculated using the following equation [24]:

$$C = \frac{1}{E_P d}\left(A + Bd\left(\frac{1}{t_P} + \frac{E_P}{E_S t_S}\right)\right)$$

where:
E_P = Young's modulus of the least stiff sheet of material in the joint.
E_S = Young's modulus of the stiffest sheet of material in the joint.
t_P = thickness of the least stiff sheet of material in the joint.
t_S = thickness of the stiffest sheet of material in the joint.
d = diameter of fasteners.
A = 1.67 and B = 0.86 for a steel bolt (these are empirical constants).

The shear stiffness of the fasteners was given by the inverse of the flexibility given above. The equation for the axial stiffness of a beam was used to calculate the axial stiffness of the fasteners:

$$K = \frac{AE}{L}$$

In this case A is the cross sectional area of the fastener and E is the fastener material's Young's modulus. L is the length the fastener acts over, which was taken as the combined thickness of the skin and stringer connected by the fasteners. The gap between the skin and stringer was ignored.

The shear and axial stiffness used for the fasteners connecting each stringer are given in Table A2. The Young's modulus assumed for the skin and stringers was 10.3×10^3 ksi and the Young's modulus assumed for the steel fasteners was 29.0×10^3 ksi. All of the other necessary dimensions may be found in Figure 2.

Table A2 - Shear and axial stiffness of the fasteners connecting each stringer to the skin.

Stringer numbers	Shear stiffness (lb/in.)	Axial stiffness (lb/in.)
4 and 8	686000	3160000
5 and 7	978000	1540000
6	612000	4190000
2, 3, 9 and 10	591000	4450000

A.3. Boundary conditions

The boundary conditions were chosen to approximate a uniform stress in both the stringers and skin of the panel. The boundary conditions are described with reference to the coordinate system used in Figure A1. The basic model, which simulated the case where all stringers are intact had the following boundary conditions:

- Edges B and D were restrained from rotating around the z axis.
- Both the skin and stringers were restrained from translation in the z direction and rotation around the x and y axis at edge A. The restraint at edge A simulates symmetry about this edge.
- All nodes (for both stringers and skin) were given a displacement of 0.25 in. in the z-direction at edge C. This was to simulate uniform stress in the panel.
- A single node at the top of all of the stringers was restrained approximately 13.5 in., 40 in., 67 in. and 100 in. from edge A. Reference 1 gave the spacing between ribs as 27 in.

The model used to simulate the panel with a splicing stringer broken had the same boundary conditions, except the end of stringer 4 at edge A was free rather than restrained. Again the model could be thought of as symmetrical about edge A, but this time there is a break in stringer 4 at its centre.

Appendix B: Results of BHEC inspections performed during the LOT inspections of A20-627 and A20-623

Table B1 - Cracks found during the BHEC inspection of stringers 4 and 8 of the left hand wing of A20-627.

Stringer	Hole row	Hole ID	Direction	Crack Type	Where[1]	Calculated depth (in.)
4	1	WS234	edge	LSEC	STIFF	0.065
4	1	WS242	centre	LSEC	STIFF	0.016
4	1	WS243	centre	LSEC	STIFF	0.008
4	1	WS244	centre	LSEC	STIFF	0.016
4	1	WS245	edge	MSEC	STIFF	0.065
4	1	WS245	centre	MSEC	STIFF	0.065
4	1	WS247	edge	TC	STIFF	0.008
4	1	WS248	centre	TC	STIFF	0.065
4	1	WS249	centre	USEC	STIFF	0.065
4	1	WS267.5	edge	LSEC	STIFF	0.065
4	1	WS541.5	edge	LSEC	STIFF	0.189
4	1	WS543	edge	LSEC	STIFF	0.376
4	1	WS544	centre	LSEC	STIFF	0.111
4	1	WS545	edge	LSEC	STIFF	0.112
4	1	WS545	centre	LSEC	STIFF	0.112
4	1	WS546.5	edge	LSEC	STIFF	0.112
4	1	WS547.5	edge	LSEC	STIFF	0.111
4	1	WS547.5	centre	LSEC	STIFF	0.111
4	1	WS553	edge	TC	STIFF	to edge
4	1	WS556	edge	LSEC	STIFF	0.111
4	2	WS297	edge	LSEC	STIFF	0.065
4	2	WS279	edge	LSEC	STIFF	0.111
4	2	WS276	edge	LSEC	STIFF	0.111
4	2	WS276	centre	LSEC	STIFF	0.111
4	2	WS269	edge	LSEC	STIFF	0.063
4	2	WS269	centre	LSEC	STIFF	0.063
4	2	WS247	centre	LSEC	STIFF	0.065
4	2	WS246	centre	LSEC	STIFF	0.065
4	2	WS541	edge	LSEC	STIFF	0.061
4	2	WS542.5	edge	LSEC	STIFF	0.081
4	2	WS544	centre	LSEC	STIFF	0.111
4	2	WS545	centre	LSEC	STIFF	0.111
4	2	WS547	edge	LSEC	STIFF	0.149

[1] STIFF indicates that the crack was in the stringer, SKIN indicates that the crack was in the skin.

Table B1 cont.

Stringer	Hole row	Hole ID	Direction	Crack Type	Where	Calculated depth (in.)
4	2	WS554	Edge	LSEC	STIFF	0.188
4	2	WS555.5	Edge	LSEC	STIFF	0.111
8	3	WS245	Edge	LSEC	STIFF	0.008
8	4	WS259	Centre	LSEC	STIFF	0.065
8	4	WS243	Centre	LSEC	STIFF	0.065
8	4	WS243	Edge	LSEC	STIFF	0.065

Table B2 - Cracks found during the BHEC inspection of stringers 5 and 7 of the left hand wing of A20-627.

Stringer	Hole row	Hole ID	Direction	Crack Type	Where	Calculated depth (in.)
5	2	WS309	edge	USEC	STIFF	0.073
5	2	WS230	centre	LSEC	STIFF	0.063
7	1	WS285.5	centre	HWC	STIFF	0.154
7	1	WS283	edge	LSEC	STIFF	0.078
7	1	WS283	centre	LSEC	STIFF	0.078
7	1	WS252.5	centre	USEC	STIFF	0.103
7	1	WS243.5	edge	USEC	SKIN	0.008
7	1	WS243.5	edge	LSEC	STIFF	0.065
7	1	WS242	edge	USEC	STIFF	0.065
7	1	WS242	centre	HWC	STIFF	0.065
7	1	WS239	edge	USEC	SKIN	0.008
7	1	WS239	centre	HWC	STIFF	0.065
7	1	WS234.5	edge	LSEC	STIFF	0.064
7	1	WS234.5	centre	HWC	STIFF	0.064
7	1	WS233	edge	USEC	STIFF	0.066
7	1	WS230	centre	USEC	STIFF	0.066

Table B3 - Cracks found during the BHEC inspection of stringers 4 and 8 of the left hand wing of A20-623.

Stringer	Hole row	Hole ID	Direction	Crack Type	Where	Calculated depth (in.)
4	1	WS216	edge	LSEC	STIFF	0.008
4	1	WS222	edge	LSEC	STIFF	0.016
4	1	WS223	edge	LSEC	STIFF	0.008
4	1	WS224	centre	LSEC	STIFF	0.015
4	1	WS224	edge	HWC	STIFF	0.015
4	1	WS226	centre	LSEC	STIFF	0.015
4	1	WS228	edge	LSEC	STIFF	0.041
4	1	WS230	centre	HWC	STIFF	0.016
4	1	WS232	edge	LSEC	STIFF	0.015
4	1	WS244	edge	LSEC	STIFF	0.015
4	1	WS245	edge	LSEC	STIFF	0.015
4	1	WS254	edge	MLSEC	STIFF	0.024
4	1	WS254	centre	HWC	STIFF	0.024
4	1	WS257	edge	LSEC	STIFF	0.033
4	1	WS263	edge	HWC	STIFF	0.008
4	1	WS264	edge	LSEC	STIFF	0.033
4	1	WS267	centre	LSEC	STIFF	0.015
4	1	WS267	edge	HWC	STIFF	0.015
4	1	WS272	edge	LSEC	STIFF	0.015
4	1	WS276	edge	LSEC	STIFF	0.007
4	2	WS212	edge	LSEC	STIFF	0.008
4	2	WS223.5	centre	LSEC	STIFF	0.015
4	2	WS261	edge	HWC	STIFF	0.032
4	2	WS266	centre	LSEC	STIFF	0.015
4	2	WS266	centre	LSEC	STIFF	0.015
4	2	WS269	centre	LSEC	STIFF	0.025
4	2	WS270	centre	LSEC	STIFF	0.041
4	2	WS523	centre	USEC	STIFF	0.008
4	2	WS544	centre	LSEC	STIFF	0.047
4	2	WS546.5	edge	LSEC	STIFF	0.016
8	4	WS261	centre	TC	STIFF	0.016
8	4	WS261	edge	TC	STIFF	0.016
8	4	WS263	edge	LSEC	STIFF	0.008

Table B4 - Cracks found during the BHEC inspection of stringers 5 and 7 of the left hand wing of A20-623.

Stringer	Hole row	Hole ID	Direction	Crack Type	Where	Calculated depth (in.)
5	2	WS229	edge	LSEC	STIFF	0.024
5	2	WS270	edge	USEC	STIFF	0.008
5	2	WS273	centre	USEC	STIFF	0.071
5	2	WS273	centre	LSEC	STIFF	0.071
5	2	WS544.5	edge	LSEC	STIFF	0.127
5	2	WS546.5	edge	LSEC	STIFF	0.206
5	2	WS547.5	edge	LSEC	STIFF	0.072
7	1	WS218	centre	LSEC	STIFF	0.072
7	1	WS218	edge	USEC	STIFF	0.072
7	1	WS220	edge	LSEC	STIFF	0.041
7	1	WS220	centre	USEC	STIFF	0.041
7	1	WS221	centre	USEC	SKIN	0.015
7	1	WS224	edge	HWKC	SKIN	0.015
7	1	WS225	centre	LSEC	STIFF	0.015
7	1	WS225	edge	USEC	STIFF	0.015
7	1	WS227	centre	LSEC	STIFF	0.015
7	1	WS231	edge	MHWC	STIFF	0.007
7	1	WS248	centre	USEC	STIFF	0.015
7	1	WS257	edge	LSEC	STIFF	0.032
7	1	WS257	centre	HWC	SKIN	0.032
7	1	WS516	edge	USEC	STIFF	0.008
7	1	WS544	centre	LSEC	STIFF	0.008

Table B5 - Codes used to describe cracks.

Code	Description
C	crack
E	edge
H	hole
K	countersink
L	lower
M	multiple
S	surface
T	through-thickness
U	upper
W	wall

DISTRIBUTION LIST

Structural Risk assessment of RAAF B707 Lower Wing Stringers

Ben Dixon

AUSTRALIA

DEFENCE ORGANISATION	**No. of copies**
Task Sponsor	
RAAF ASI: L. Grey	2
S&T Program	
Chief Defence Scientist FAS Science Policy AS Science Corporate Management Director General Science Policy Development	Shared
Counsellor Defence Science, London	Doc Data Sht
Counsellor Defence Science, Washington	Doc Data Sht
Scientific Adviser Joint	1
Navy Scientific Adviser	Doc Data Sht & Dist List
Scientific Adviser – Army	Doc Data Sht & Dist List
Air Force Scientific Adviser	Doc Data Sht & Dist List
Scientific Adviser to the DMO	Doc Data Sht & Dist List
Scientific Adviser to the DMO ELL	Doc Data Sht & Dist List
Platforms Sciences Laboratory	
Chief, AVD	Doc Data Sht & Dist List
Research Leader Aircraft Structures, G. Clark	1
Head, Risk and Reliability: K. Watters	1
Author: B. Dixon	1
L. Meadows	1
P. Jackson	1
DSTO Library and Archives	
Library Fishermans Bend	1
Library Edinburgh	1
Defence Archives	1
Capability Development Group	
Director General Maritime Development	Doc Data Sheet
Director General Capability and Plans	Doc Data Sheet
Assistant Secretary Investment Analysis	Doc Data Sheet
Director Capability Plans and Programming	Doc Data Sheet
Director General Australian Defence Simulation Office	Doc Data Sheet
Director Trials	Doc Data Sheet

Chief Information Officer Group

Director CIO	Doc Data Sheet
Director General Information Policy and Plans	Doc Data Sheet
AS Information Strategy and Futures	Doc Data Sheet
AS Information Architecture and Management	Doc Data Sheet
Director General Australian Defence Simulation Office	Doc Data Sheet
Director General Information Services	Doc Data Sheet

Strategy Group

Director General Military Strategy	Doc Data Sheet
Director General Preparedness	Doc Data Sheet
Assistant Secretary Strategic Policy	Doc Data Sheet
Assistant Secretary Governance and Counter-Proliferation	Doc Data Sheet

Navy

SO (SCIENCE), COMAUSNAVSURFGRP, NSW	Doc Data Sht & Dist List
Maritime Operational Analysis Centre, Building 89/90 Garden Island Sydney NSW	
Deputy Director (Analysis)	Doc Data Sht & Dist List
Director General Navy Capability, Performance and Plans, Navy Headquarters	Doc Data Sheet
Director General Navy Strategic Policy and Futures, Navy Headquarters	Doc Data Sheet

Air Force

SO (Science) - Headquarters Air Combat Group, RAAF Base, Williamtown NSW 2314	Doc Data Sht & Exec Summ

Army

SO (Science) - Land Headquarters (LHQ), Victoria Barracks NSW	Doc Data & Exec Summary
SO (Science), Deployable Joint Force Headquarters (DJFHQ) (L), Enoggera QLD	Doc Data Sheet

Joint Operations Command

Director General Joint Operations	Doc Data Sheet
Chief of Staff Headquarters Joint Operations Command	Doc Data Sheet
Commandant ADF Warfare Centre	Doc Data Sheet
Director General Strategic Logistics	Doc Data Sheet

Intelligence and Security Group

DGSTA , Defence Intelligence Organisation	1
Manager, Information Centre, Defence Intelligence Organisation	1 (PDF)
Assistant Secretary Capability Provisioning	Doc Data Sheet
Assistant Secretary Capability and Systems	Doc Data Sheet
Assistant Secretary Corporate, Defence Imagery and Geospatial Organisation	Doc Data Sheet

Defence Materiel Organisation

Deputy CEO	Doc Data Sheet
Head Aerospace Systems Division	Doc Data Sheet
Head Maritime Systems Division	Doc Data Sheet
Chief Joint Logistics Command	Doc Data Sheet
Head Materiel Finance	Doc Data Sheet

Defence Libraries

Library Manager, DLS-Canberra	1
Library Manager, DLS – Sydney West	Doc Data Sheet

SPARES	2

Total number of copies: 17 **Printed: 16** **PDF: 1**

DEFENCE SCIENCE AND TECHNOLOGY ORGANISATION

DOCUMENT CONTROL DATA

1. PRIVACY MARKING/CAVEAT (OF DOCUMENT)

2. TITLE

Structural Risk Assessment of RAAF B707 Lower Wing Stringers

3. SECURITY CLASSIFICATION (FOR UNCLASSIFIED REPORTS THAT ARE LIMITED RELEASE USE (L) NEXT TO DOCUMENT CLASSIFICATION)

Document	(U)
Title	(U)
Abstract	(U)

4. AUTHOR(S)

B. Dixon

5. CORPORATE AUTHOR

Platform Sciences Laboratory
506 Lorimer St
Fishermans Bend Victoria 3207 Australia

6a. DSTO NUMBER	6b. AR NUMBER	6c. TYPE OF REPORT	7. DOCUMENT DATE
DSTO-TR-1741	AR-013-448	Technical Report	July 2005

8. FILE NUMBER	9. TASK NUMBER	10. TASK SPONSOR	11. NO. OF PAGES	12. NO. OF REFERENCES
2005/1030331/1	03/192	RAAF ASI: L. Grey	58	24

13. URL on the World Wide Web

http://www.dsto.defence.gov.au/corporate/reports/DSTO-TR-1741.pdf

14. RELEASE AUTHORITY

Chief, Air Vehicles Division

15. SECONDARY RELEASE STATEMENT OF THIS DOCUMENT

Approved for public release

OVERSEAS ENQUIRIES OUTSIDE STATED LIMITATIONS SHOULD BE REFERRED THROUGH DOCUMENT EXCHANGE, PO BOX 1500, EDINBURGH, SA 5111

16. DELIBERATE ANNOUNCEMENT

No Limitations

17. CITATION IN OTHER DOCUMENTS Yes

18. DEFTEST DESCRIPTORS

Aircraft structures, Probability theory, Service life, Reliability engineering.

19. ABSTRACT

This report details a structural risk assesment of the critical lower wing stringers in RAAF B707 aircraft. The analysis uses condition data from sampling inspections of RAAF aircraft to describe possible cracking of these stringers in the fleet. It then uses crack growth and load exceedance data that has been adapted from a USAF risk assessment of the B707 to predict the future probability of failure of the B707 lower wing.